CHARACETERIZATION OF PHOTORECEPTOR-CONTROLLED AGGREGATION AND DISAGGREGATION OF MICROPARTICLE SUSPENSIONS.

by

Christopher B. Cone

July, 2021

Director of Thesis: Loren Limberis

Major Department: Engineering

ABSTRACT

Phytochromes are a unique classification of photoreceptors used by plants to perceive light for many physiological processes. Phytochrome B (PhyB) possesses two interconvertible forms which can be activated under specific wavelengths of light to bind and unbind an integrating factor PIF3 to carry out gene expression within the nucleus of plant cells. This natural switching mechanism of PhyB to bind and unbind PIF3 provides the potential to create a photo-switchable controlling mechanism as a platform for biotechnological devices. The overall goal of this research was to develop a platform using microparticles coated with PhyB and PIF3 proteins that would interact under the control of light by aggregating and disaggregating based on wavelength, intensity, and duration of light.

The development of a microparticle-based platform to immobilize these photoreactive protein counterparts presents many challenges. To express photoresponsive recombinant PhyB protein in *E. coli* cells, two additional proteins are required to be coexpressed that are toxic to the cells. In addition, expression levels of soluble and active PhyB are very low (around 15%) and must be produced under dark room conditions. Another challenge is to immobilize the PhyB and PIF3 proteins on surfaces that retains their photo-responsive attributes and can interact as part of

the device platform. Further challenges are the characterization of these photo-responsive interactions between PhyB and PIF3 to determine the operating conditions and limitations in developing this platform.

Truncated versions of PhyB and PIF3 were expressed using benchtop bioreactors and purified using affinity chromatography. The proteins were characterized as freely suspended proteins in solution as well as immobilized on treated polystyrene microparticle surfaces and agarose-coated magnetic particles. The proteins were also characterized by their interactions in which one protein was in suspension while the counterpart protein was immobilized on a microparticle. The interactions between separately-coated protein particles, the essence of the proposed platform, was also investigated. Despite the expected low yields, the purified PhyB protein displayed photo-responsive characteristics based the wavelength of light used (red light, 660 nm for active and far-red light, 730 nm for inactive) as well as dark reversion kinetics (the protein in the active state reverting to its inactive state without photoinduction). However, when immobilized on polystyrene particles or magnetic particles, PhyB seemed to lose its photo-responsiveness, or at least couldn't bind to PIF3 while immobilized and in the active state. Based on gel electrophoresis analysis, the immobilization of truncated PhyB to microparticles seemed to affect the binding of PIF3 in solution when the truncated PhyB was irradiated with red light. On the other hand, depletion assays indicated immobilized PhyB was able to bind and unbind suspended PIF3 in the two photoinduced states. Depletion assays also indicated a more photo-responsive interaction when PIF3 was immobilized on the bead surface while PhyB remained suspended in solution. To test the hypothesis of the platform, aggregation and disaggregation experiments where both proteins were immobilized on separate microparticles were conducted and observed by light microscopy. No aggregation was observed under photoactive red light

conditions. The overall results seem to indicate the truncated versions of PhyB and PIF3, while displaying photo-responsive activity in suspension, are inhibited when specifically immobilized on microparticle surfaces.

CHARACTERIZATION OF PHOTORECEPTOR-CONTROLLED AGGREGATION AND DISAGGREGATION OF MICROPARTICLE SUSPENSIONS.

A Thesis

Presented to the Faculty of the Department of Engineering

East Carolina University

In Partial Fulfillment of the Requirements for the Degree

Master of Science in Biomedical Engineering

by

Christopher B. Cone

July, 2021

CHARACTERIZATION OF PHOTORECEPTOR-CONTROLLED AGGREGATION AND DISAGGREGATION OF MICROPARTICLE SUSPENSIONS.

by

Christopher B. Cone

APPROVED BY:

DIRECTOR OF
THESIS:

_____

Loren Limberis, PhD

COMMITTEE MEMBER:

_____

Ali Vahdati, PhD

COMMITTEE MEMBER:

_____

Xin-Hua Hu, PhD

CHAIR OF THE DEPARTMENT
OF (Engineering):

_____

Barbara Muller-Borer, PhD

DEAN OF THE
GRADUATE SCHOOL:

_____

Paul J. Gemperline, PhD

TABLE OF CONTENTS

LIST OF TABLES

LIST OF FIGURES

CHAPTER 1: INTRODUCTION

Light is a source of energy and information for plants. Plants perceive light signals based on intensity, wavelength, and duration of irradiance. Several photoreceptors are involved in the perception of these light signals which gather information to guide physiological processes. One classification of photoreceptors are phytochromes, which exist mainly in two interconvertible forms, one with maximum absorption in red light and another with maximum absorption in far-red light (1). One phytochrome protein PhyB changes conformation under these conditions and, based on wavelength and irradiance information, it will conform to an active or inactive form in which it can control the binding and unbinding of the phytochrome interactive factor PIF3 (1). When PhyB is in its active form, it will bind to PIF3 to initiate a signaling pathway for specific genetic expression. Once irradiated with far-red light, PhyB will change conformation to its inactive form and release PIF3 to cease expression. This photo-reversible switching mechanism using light signals could provide potential applications in biotechnology and nanobiological devices. The switching mechanism of these photosensitive devices could be dynamically controlled based on light intensity, wavelength, and duration of irradiance. The different wavelengths of light could control the active/inactive states of the protein complex; the intensity of light could control the concentration of photoreceptor proteins activated; and the duration of irradiance could maintain steady-state conditions to account for dark reversion of active form passively converting to inactive form. The objective of this study is to integrate the photo-reversible protein complex of PhyB and PIF3 into a light switching control mechanism as a platform for nanobiotechnology applications.

The overall design of the switching control mechanism is based on the hypothesis that a colloidal suspension of a mixture of PhyB-coated particles and PIF3-coated particles irradiated

with red light will assemble into an aggregate. This aggregate can then disassemble by irradiating the solution with far-red light. The on/off dynamics (aggregation/disaggregation) of the protein complex can be controlled by light intensity, wavelength, and duration of irradiance. This photo-switchable controlling protein complex offers the potential for a variety of devices with applications in biosensors, nanodevices, instrumentation, and microfluidic devices. For example, the switching control mechanism of the PhyB/PIF3 complex could be integrated into a chromatography system to elute molecules of interest or even build unique structures at the micro-level all based on light control.

CHAPTER 2: BACKGROUND

Phytochromes are a family of plant sensory photoreceptors designated as PhyA through PhyE (2). Their function is to monitor environmental information such as light conditions to regulate plant signaling pathways for plant growth development, seed germination, flowering, and other plant responses (1, 2). The phytochromes regulate the signaling pathways through conformational active and inactive forms based upon light intensity, wavelength, and irradiance duration. These conformational active and inactive forms of phytochromes are regulated when irradiated with red and far-red light, respectively. When irradiated with red light, the phytochrome conforms to its active state to trigger signal transduction pathways to alter gene expression through transcriptional networks. Once the phytochrome is irradiated with far-red light, it will revert to its inactive form and cease gene expression.

The most studied and characterized plant phytochrome family member is phytochrome B (PhyB), which is the main light receptor responsible for the shade avoidance response in mature plants (2). Its three-dimensional structure consists of a homodimer with chains A and B at a molecular weight of around 129 kDa as shown in Figure 1 (3).

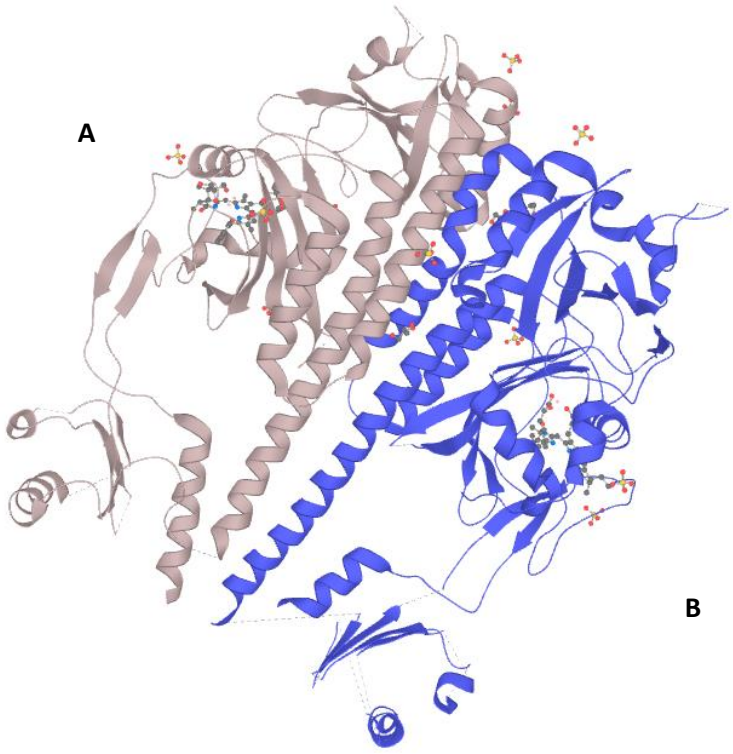

Figure 1. Three-dimensional structure of the homodimer PhyB (3). PhyB consists of two chains A and B which interact to bind to phytochrome interacting factors.

This homodimer structure allows the two chains A and B to interact with each other when irradiated with light at 740 nm and 660 nm to reversibly fold into two stable conformers called Pr (red light absorbing) and Pfr (far-red light absorbing) as shown in Figure 2.a (1). Phytochromes subside in the cytoplasm in their inactive Pr form. Once exposed to red light, the phytochrome conforms to its active Pfr form and can begin signal transduction. When irradiated with red light the two chains A and B fold into the Pfr form to bind a signaling partner phytochrome interacting factor PIF3 to carry out physiological and developmental processes as shown in Figure 2.b.

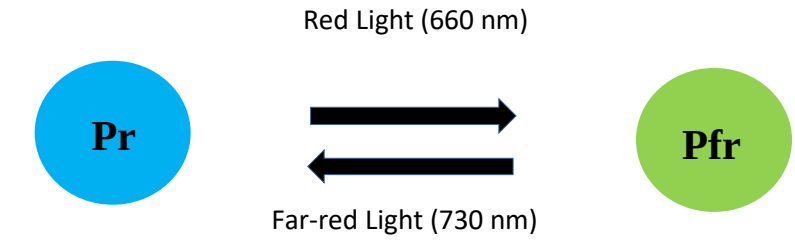

(a).

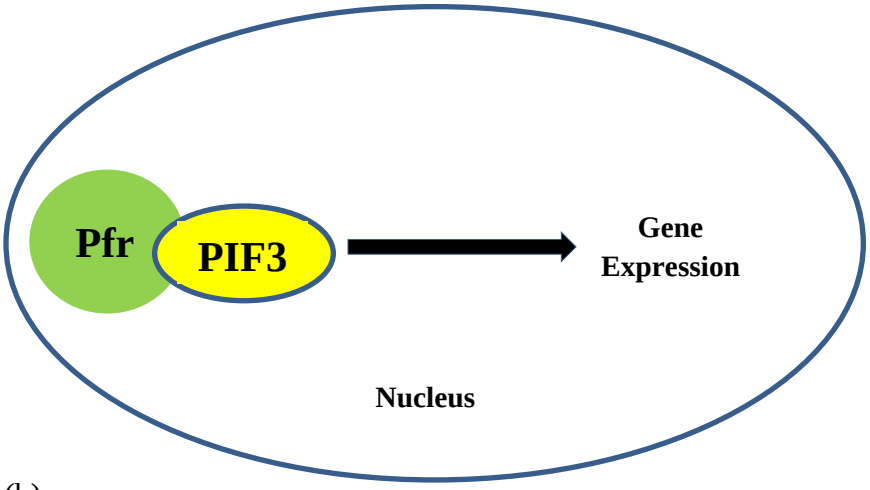

(b).

Figure 2. Light absorbing conformers and signaling pathway for PhyB Protein. (a) PhyB can switch its conformation reversibly upon irradiance of red (Pfr) and far-red light (Pr). (b) Signaling pathway for PhyB. Upon irradiance of red light, PhyB will enter the nucleus to interact with PIF3 to initiate gene expression.

PIF3 is a basic helix-loop-helix protein which can bind to the carboxy-terminal fragments of phytochromes, specifically phytochrome A and B (4). It binds to a G-box DNA sequence motif which is present in various light regulated promoters (5, 6). As shown in Figure 2.b, PIF3 localizes in the nucleus of cells and is a transcriptional regulator for phytochrome signaling to photoregulated genes (7). The three-dimensional structure of PIF3 is also a homodimer with chains A and C at a molecular weight of around 57 kDa as shown in Figure 3 (8). The basic structure and characteristics of PhyB and PIF3 have made it possible to study these proteins *in*

.

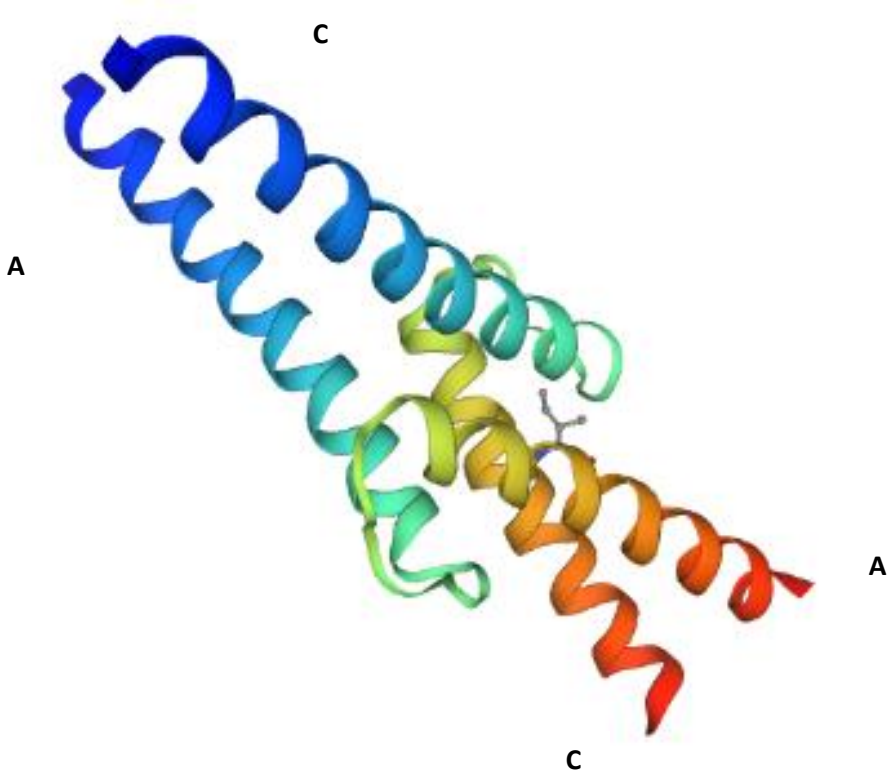

Figure 3. Three-dimensional structure of PIF3 (8). The homodimer PIF3 contains two chains A and C.

vitro and use the photo-switchable regulatory control of the PhyB/PIF3 complex to create a platform for nanobiological devices

Previous Research

PhyB and PIF3 have been well characterized for their physiological functions in plants and photosensitive activity *in vitro*. Over the years, phytochrome characteristics such as absorption spectra, fluence and irradiance response, structural orientation, functionality, signaling, degradation, etc. have been studied (9). Binding efficiency of PhyB and PIF3 has been analyzed along with binding reaction when PIF3 is immobilized on agarose beads and then

saturated with PhyB (10). PhyA and PhyB have both been tested *in vitro* with PIF3 and PhyB has a higher affinity to PIF3 than PhyA and also PhyB is more stable in its active Pfr form than other phytochromes (9, 10). PhyB has also been studied through its assembly with phytochromobilin (PΦB), photointerconversion between Pr and Pfr, thermal reversion from Pfr back to Pr, aggregation into nuclear bodies after irradiation with red light, degradation upon far-red light irradiation, and stimulation of photomorphogenic processes fully or partially controlled by PhyB (11). This phytochromobilin assembly with PhyB in *E coli* illustrated protein folding and bilin conjugation was not compromised during expression. Thermal reversion from Pfr back to Pr refers to the light-independent relaxation (dark reversion) of the thermodynamically less stable Pfr into the Pr conformer. The implication is that dark reversion can play an important role under conditions when the amount of the Pfr form is limited for instance in low-fluence nonsaturating light. (1, 12). Zhang et al showed PhyB would form PhyB bodies in the nucleus upon red light irradiation and would also naturally degrade to its inactive state when irradiated with far-red light. The PhyB plants were rescued with various PhyB mutants to photo-morphogenic processes controlled by PhyB (11). These well-defined characteristics of PhyB and its interaction with PIF make it possible to create a suitable platform for nanobiological devices with photosensitive and photo-reversible control.

To fully characterize the photo-interactions of recombinant versions of PhyB and PIF3 *in vitro* for use in a photo-controllable device platform, large quantities of each protein must be produced and purified. However, the expression of photosensitive recombinant PhyB does require several interacting components (Figure 4): the expression of recombinant apo-PhyB (phytochrome without the chromophore, PΦB); the conversion of heme to biliverdin by heme oxygenase (HO1); the conversion of biliverdin to chromophore PΦB by PΦB synthase (HY2);

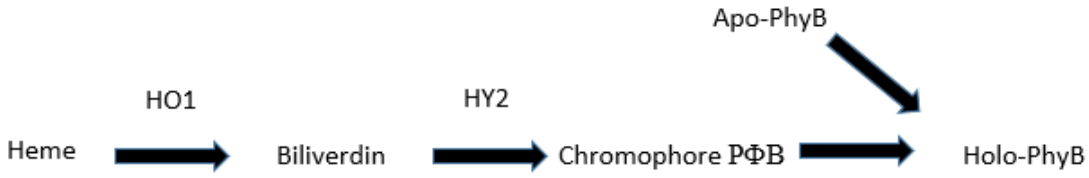

Figure 4. Synthesis process for holo-PhyB. Heme oxygenase (HO1) converts heme to biliverdin. PΦB synthase (HY2) then converts Biliverdin to the phytochromobilin PΦB. Apo-PhyB is co-expressed with the PΦB to form holo-PhyB.

and the covalent attachment of PΦB to apo-PhyB to form the photo-responsive protein holo-PhyB. Expressing recombinant holo-PhyB protein in *E. coli* requires three different plasmids (heme oxygenase, PΦB synthase, and PhyB) and this type of triple-transformed *E. coli* presents certain challenges. First challenge is heme oxygenase and PΦB synthase are toxic to *E. coli* at high concentrations which can cause low expression during production of PhyB. Low concentration of the HO1 and HY2 plasmid will need to be expressed along with the chromophore PΦB to achieve a photo-responsive holo-PhyB. A photo-responsive holo-PhyB has been expressed in *E. coli* under *in vitro* conditions (13), but the apo-PhyB has been shown to cause low expression and insolubility issues in *E. coli* (14). According to Mukougawa 2006, the covalent attachment of PΦB to apo-PhyB to form the photo-responsive protein holo-PhyB recorded a yield of 3.3 mg/L which was considerably higher than the apo-PhyB yield (13). Therefore, the holo-PhyB protein will need to be overexpressed under controlled conditions such as pH, temperature, stir rate, dissolved oxygen, and even filtered light to achieve a high PhyB yield and maintain the inactive and more stable Pr form of PhyB.

This photo-controllable mechanism between PhyB and PIF3 has only been used in few applications. One application of the photoinduced system was the development of a light-switchable gene promoter system (15). This application used two fusion proteins consisting of

PhyB/GAL4-DNA-binding domain and PIF3/GAL4-activation-domain to activate the GAL4 protein. This photo-controllable system has also been used to explore actin assembly photoswitching (16). Once again, PhyB and PIF3 were used as fusion proteins to activate the Wiskott-Aldrich Syndrome Protein (WASP) to stimulate actin assembly. Most recently, photoregulatory protein kinases have been established as critical components in catalyzing the photoactivated-phy-induced phosphorylation of PIF3 *in vivo* (17). These photoregulatory protein kinases were shown to regulate plant growth and development in response to multiple signaling pathways.

Overall, these reported applications utilize the photoregulatory components of PhyB and PIF3 as a signaling pathway to assist with biological processes and to control these processes via light signals. This proposed research takes a different approach to applying the PhyB/PIF3 photo-controllable mechanisms, not by controlling expression in systems or activation of actin assembly systems, but rather applying the photo mechanisms for an overall platform with the goal of developing different types of biotechnology devices. The proposed platform applies these photo-characteristics of PhyB and PIF3 to provide the framework for a photoregulatory switching device by controlling the aggregation and disaggregation of a colloidal suspension of PhyB and PIF3 microparticles.

The implication that specific plant physiology is controlled by red and far-red light as part of the PhyB/PIF3 system is another rationale for the hypothesized platform in which aggregation and disaggregation of microparticles can be controlled using a recombinant version of the PhyB/PIF3 system by various lighting conditions. The in vitro reconstitution of the PhyB/PIF3 system for the proposed device platform requires the immobilization of PhyB and PIF3 on non-biological surfaces. However, controlling protein interaction on a nonbiological

surface is a challenge in the biological and biotechnology fields. When proteins interact with surfaces such as glass, metals, and plastics, they typically denature on the surface and lose their three-dimensional structure and their biological function. For the proposed platform to work well surface chemistry modifications on non-biological surfaces will be required to mimic the natural characteristics of a biological surface. Ideally, these modifications need to allow for specific immobilization of the proteins in a way to maintain their secondary and tertiary structures, and hence, their biological activity. An ideal surface would also have the ability to prevent surface fouling and inhibit non-specific binding. Several approaches for modifying non-biological surfaces to mimic physiological surfaces can be found in the extensive literature associated with increasing the biocompatibility of biomaterials for the medical and biotechnology fields. One promising surface modification is the use of surfactants, such as Pluronic surfactants. These surfactants are triblock copolymers comprised of two poly(ethylene oxide) (PEO) terminal segments with a central segment of poly(propylene oxide) (PPO). They exhibit an amphiphilic character in aqueous solution in which the PEO blocks are hydrophilic, while the PPO blocks are hydrophobic (18). The PPO blocks can interact and essentially attach to a hydrophobic surface such as a polystyrene bead as shown in Figure 5. This allows the PEO segments to extend into solution from the polystyrene beads to inhibit protein interaction on the surface. These Pluronic surfactants have been used in industry and research due to their ability to control surface fouling and improve biocompatibility (18, 19).

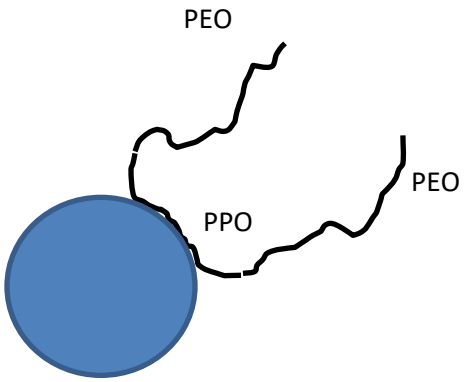

Figure 5. Pluronic surfactant on polystyrene bead. Hydrophobic PPO interacts with the hydrophobic surface of the polystyrene beads leaving the hydrophilic PEO segments extending into solution.

Pluronic surfactants can also be chemically modified to feature terminal binding groups for specific immobilization of tagged molecules. Not only will the surfactant provide the advantages of preventing surface fouling and non-specific immobilization of proteins, the modified Pluronic can also extend the terminal binding moieties into solution to specifically bind to certain features (tags) of proteins and other molecules. One particular molecule added to a Pluronic surfactant (Pluronic F108) is a metal chelating nitrile triacetic acid (NTA) which assists with the binding of histidine-tagged proteins (20). Six histidine amino acid residues genetically appended to either the carboxyl- or amino-terminus of recombinant proteins can be used as "handles" to bind the imidazole feature of histidine to a chelated metal ion. This metal chelating Pluronic surfactant (F108-NTA) has been successfully used to specifically immobilize histidine-tagged firefly luciferase on polystyrene microspheres. The immobilized bioluminescent enzyme showed 93% retention of its bioluminescent activity (20). Therefore, using a metal-chelating Pluronic surfactant F108-NTA will enable the ability to immobilize recombinant histidine-tagged PhyB and PIF3 on hydrophobic polystyrene microparticles (Figure 6).

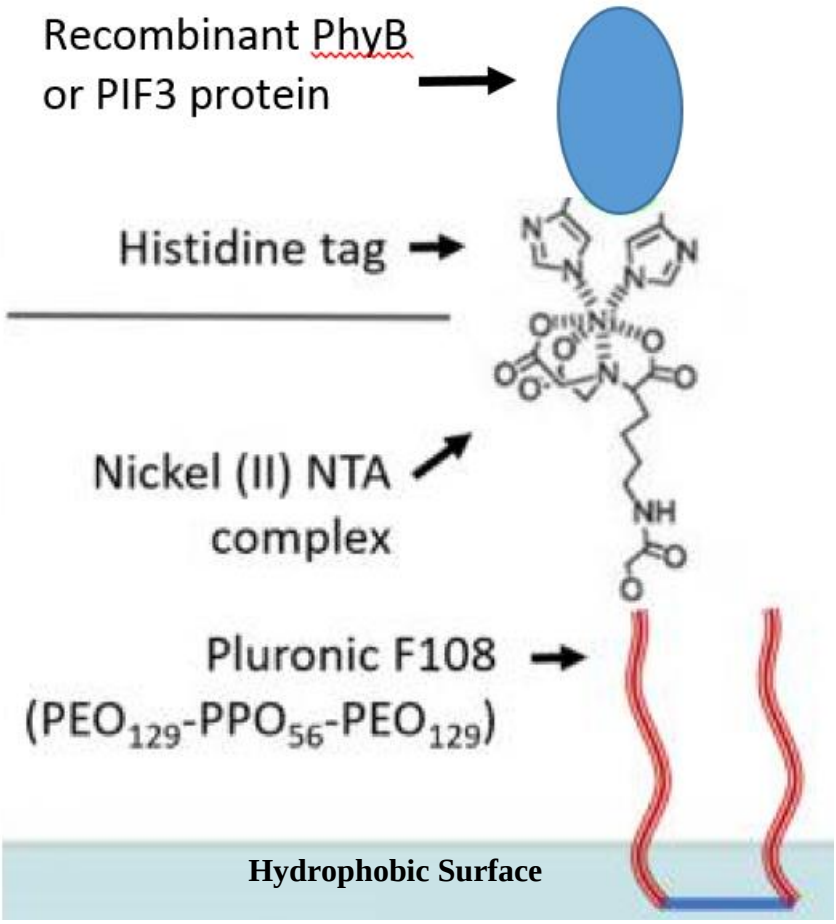

Figure 6. PhyB or PIF3 immobilized on Pluronic surfactant F108-NTA (21). PPO_{56} interacts with a hydrophobic surface while the hydrophilic PEO_{129} chains extend into solution to allow the Ni^{2+} NTA complex to bind to the histidine tagged PhyB or PIF3.

CHAPTER 3: SPECIFIC AIMS

The overall hypothesis for this study is that a colloidal suspension of two sets of particles one with immobilized PhyB and the other immobilized PIF3 when irradiated with red and far-red light will aggregate and disaggregate respectively (Figure 7). The use of the metal-chelating Pluronic surfactant F108-NTA on polystyrene beads would allow for unique structures to be created as crosslinking would occur between PhyB and PIF3 beads since the bead surface is covered with a monolayer of each protein. Therefore, the Specific Aims for this project will be based on the design and analysis of photo-controllable microparticle suspensions.

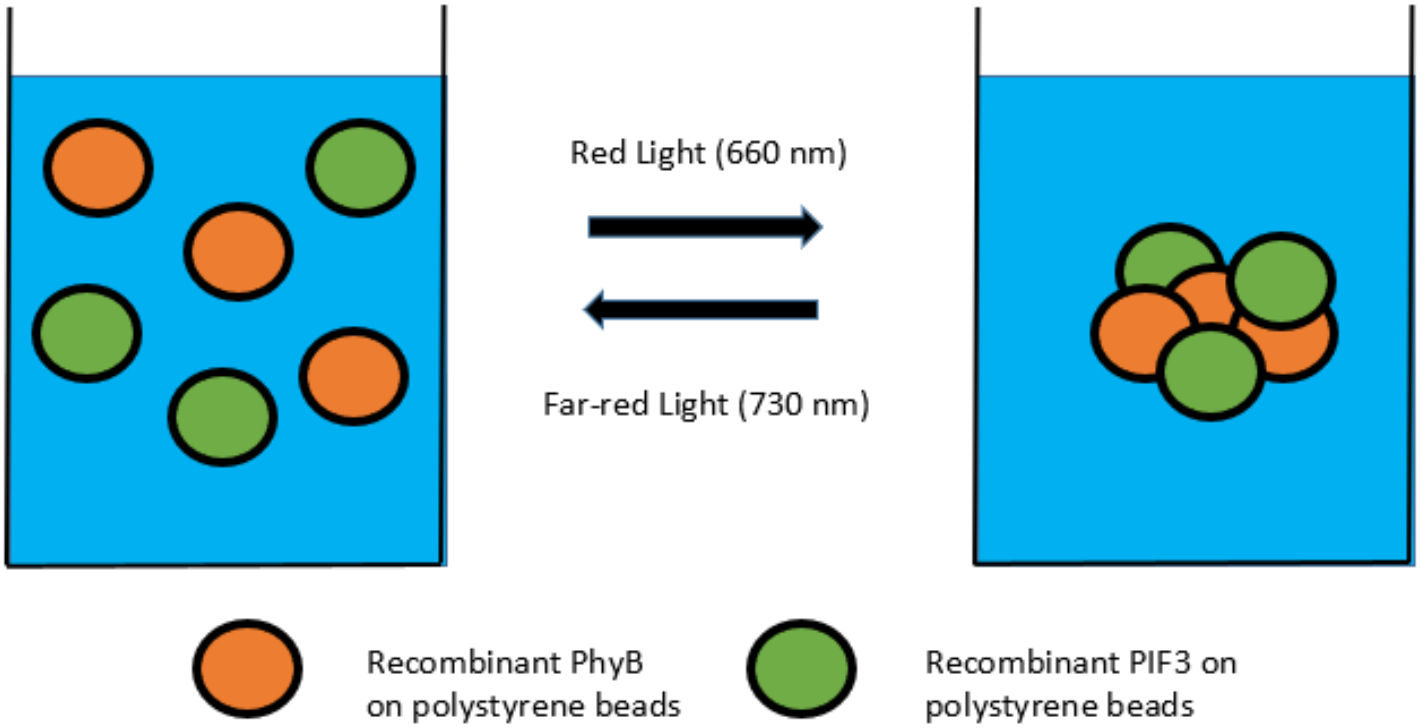

Figure 7. Aggregation and disaggregation of PhyB and PIF3 coated nanoparticles. Aggregation will occur when PhyB is irradiated with red light which will initiate the binding of PIF3 to cause crosslinking between different particles. Disaggregation will occur when the colloidal suspension is irradiated with far-red light which will induce PhyB to switch to its inactive conform and release PIF3.

The experimental design for each Specific Aim is detailed below to reach the conclusion for the overall hypothesis.

Specific Aim 1. Perform triple-transformation of plasmids for apo-PhyB, heme oxygenase, and PΦB synthase in *E. coli* BL21(DE3) cells. Design growth conditions in bioreactor, and overexpress and purify recombinant PhyB. Express and purify PIF3.

A triple transformation *E. coli* cell stock for expressing holo-PhyB is available in the East Carolina University Bioprocess Engineering Laboratory. The triple-transformed cell stock consists of a histidine-tagged apo-PhyB, heme oxygenase (HO1), and phytochromobilin PΦB synthase lacking the transient peptide (ΔHY2) (14) and are coexpressed in BL21(DE3) *E. coli* to make a holo-PhyB product. Production of holo-PhyB will be done using 5L benchtop bioreactors from Sartorius which are available in the Bioprocess Engineering Laboratory. Production in the bioreactor provides a controllable environment for growth conditions and IPTG induced expression to achieve high cell growth volumes and protein yields compared to shake flask cultures. This will provide an overexpression of the holo-PhyB protein to work with to overcome the challenges of low expression levels of apo-PhyB in *E. coli* and treating the cells with three different antibiotics. The histidine-tagged PhyB will be purified using immobilized metal ion affinity chromatography (IMAC). PhyB purification procedures will be done under cold room conditions to stabilize the proteins and under filtered green light "dark room conditions" to maintain the Pr form (the more stable, inactive form). Bioreactor cultures will be harvested by centrifugation and then lysed by sonication. The PhyB cell lysate will be loaded onto a Ni-NTA agarose column and then eluted with increasing concentrations of imidazole. The imidazole competes with the chelated Ni^{2+} ions to help elute the purified PhyB. Therefore, the imidazole will need to be removed from the purified PhyB using a Sephadex based buffer

exchange column (GE Lifesciences PD-10). The purified PhyB will be flash frozen in liquid nitrogen and stored at –80^{o}C for preservation. SDS-PAGE analysis will be used to test purity of the purified PhyB and a Bradford assay with a BSA standard will be used to determine the concentration of the purified PhyB.

Production of PIF3 will be controlled in a 5L bioreactor, but the PIF3 plasmid is a single transformation under ampicillin resistance and IPTG inducible in *E. coli*. This PIF3 protein also contains a histidine-tag and will be purified and analyzed under the same method as PhyB.

Specific Aim 2. Characterize recombinant PhyB in solution.

The following measurements will be taken to characterize the photosensitive activity of the purified recombinant PhyB:

Absorption spectra and difference spectra: The absorbance spectra of the Pr and Pfr form of PhyB will be measured between 300 nm and 1000 nm using a dual-beam UV-VIS-IR spectrophotometer. This will determine the wavelength dependence of absolute molar absorption coefficients and difference spectra for the PhyB inactive and active forms. The optimal wavelength from these absorbance spectra will be identified for protein activation. A xenon light source with interference wavelength filters will be used to activate the phytochromes and induce inactive and active PhyB conforms. Spectral scans for each conform will be done to determine their respective absorption wavelengths and to assist with determining the maximum and minimum absorption wavelengths of the difference spectra for each conform.

Light irradiance sensitivity: The intensity of light can likely affect the conformational changes of the proteins. Therefore, the irradiance of incident light could help determine the density of photons in the colloidal suspension. The use of neutral density filters to control the intensity of

light will assist with measuring conformational changes of the protein when examining their absorbance spectra.

Dark reversion kinetics: A significant factor toward the development of photo-controllable devices using the PhyB/PIF3 complex is the passive reversion of PhyB active form (Pfr) to inactive form (Pr). Thermal reversion from Pfr back to Pr refers to the light-independent relaxation (dark reversion) of the thermodynamically less stable Pfr into the Pr conformer. Understanding the dark reversion kinetics of PhyB will provide information on the steady-state conditions of the active Pfr conform. To analyze the dark reversion kinetics, the PhyB protein will be measured by using saturated red light conditions and absorption spectra. This will help determine the ratio of the absorbance changes at the peak wavelengths and therefore provide information on maintaining steady-state conditions for the active Pfr form of PhyB.

Specific Aim 3. Characterize PhyB on polystyrene beads with PIF3 in solution.

The photoregulated interaction between PhyB and PIF3 proteins will be characterized through adjusting the wavelength of light. The interaction between PhyB and PIF3 will be analyzed by adding PIF3 to an immobilized PhyB. Two conditions will be examined. First, PIF3 binding to immobilized PhyB will be characterized. Second, the unbinding or release of PIF3 from immobilized PhyB will be characterized. These experiments are detailed below:

Binding of PIF3 to PhyB: The histidine-tagged PhyB will be specifically immobilized on F108-NTA-Ni^{2+} coated polystyrene nanoparticles and irradiated with far-red light to induce the inactive Pr conformation. PIF3 protein will then be added to the PhyB suspensions. The suspensions will then be irradiated with red light to induce binding of PIF3 to PhyB. Another suspension will receive no light to represent a control. The control and test suspensions will be

pelleted by centrifugation and the protein content in the pellets and supernatants will be analyzed through SDS-PAGE analysis. The concentration of PIF3 in the supernatant will be measured by using a Bradford assay with BSA standard.

Release of PIF3 from PhyB: The histidine-tagged PhyB will be specifically immobilized on F108-NTA-Ni^{2+} coated polystyrene nanoparticles and irradiated with red light to induce the active Pfr conformation. PIF3 protein will then be added to the PhyB suspensions. The suspensions will then be irradiated with far-red light to release PIF3 from PhyB. Another suspension will receive no light to represent a control. The control and test suspensions will be pelleted by centrifugation and the protein content in the pellets and supernatants will be analyzed through SDS-PAGE analysis. The concentration of PIF3 in the supernatant will be measured by using a Bradford assay with BSA standard.

Specific Aim 4. Characterize PIF3 on polystyrene beads with PhyB in solution.

This specific aim will follow the same procedure as specific aim 3, but PIF3 will now be immobilized with the addition of PhyB protein in solution. This will help determine the photo-responsive interaction between PhyB and PIF3 and compare the photoactivity of each immobilized protein when the other is free in solution. Detailed procedures are stated below:

Binding of PhyB to PIF3: The histidine-tagged PIF3 will be specifically immobilized on F108-NTA-Ni^{2+} coated polystyrene nanoparticles and the inactive Pr form of PhyB will be added to the suspension. This will then be irradiated with red light to induce an active Pfr conformation of PhyB. Another suspension will receive no light to represent a control. The control and test suspensions will be pelleted by centrifugation and the protein content in the pellets and

supernatants will be analyzed through SDS-PAGE analysis. The concentration of PhyB in the supernatant will be measured by using a Bradford assay with BSA standard.

Release of PhyB to PIF3: The histidine-tagged PIF3 will be specifically immobilized on F108-NTA-Ni^{2+} coated polystyrene nanoparticles and the active Pfr form of PhyB will be added to the suspension. This will then be irradiated with far-red light to induce an inactive Pr conformation of PhyB. Another suspension will receive no light to represent a control. The control and test suspensions will be pelleted by centrifugation and the protein content in the pellets and supernatants will be analyzed through SDS-PAGE analysis. The concentration of PhyB in the supernatant will be measured by using a Bradford assay with BSA standard.

Specific Aim 5. Characterize photo-induced aggregation and disaggregation of polystyrene nanoparticle suspensions.

The overall goal for this project is to develop and characterize a colloidal suspension of PhyB and PIF3 which when irradiated with red and far-red light will aggregate and disaggregate, respectively. To achieve this goal, the transient state dynamics and steady state conditions for light-induced aggregation, light-induced disaggregation, dark reversion-based disaggregation, and pulse with modulation of concurrent red and far-red light to maintain intermediate levels of aggregation will need to be characterized. Each procedure is detailed below:

Characterize red light-induced aggregation dynamics: The aggregation dynamics of the colloidal suspension will be analyzed by two approaches: imaging it at low concentrations and measuring optical density at high concentrations. To image the colloidal suspension at low nanoparticle concentrations, the use of glass depression slides and an inverted microscope will be used. Two images for each sample will be taken at different wavelengths. These wavelengths

are based off the maximum and minimum absorption spectra of the PhyB and not the red and far-red wavelengths for conformational switching. To remove background noise and achieve optimal image contrast, differential images will be taken from the two images. These two images will allow for the quantification of aggregated colloidal suspensions as a function of time and red light irradiance. Measuring the optical density (turbidity in this case) using a spectrophotometer of the colloidal suspensions at high concentrations will provide a quantifiable aggregation as a function of time and red light irradiance.

Experimental conditions such as pH, temperature, viscosity, nanoparticle concentration, etc. will be investigated to characterize the dynamics of PhyB/PIF3 aggregation. The suspensions of PhyB/PIF3 nanoparticles will be saturated with far-red light to induce an inactive conformation of PhyB to achieve steady state and then irradiated with red light to initiate aggregation.

Characterize far-red light-induced disaggregation dynamics: The disaggregation dynamics of the colloidal suspension will be analyzed with the same experimental approach as in the aggregation dynamics. Differential images and spectrophotometric measurements will be used to quantify disaggregation based off time and far-red light irradiance. Experimental conditions such as pH, temperature, viscosity, nanoparticle concentration, etc. will be investigated to characterize the dynamics of PhyB/PIF3 disaggregation. The suspensions of PhyB/PIF3 nanoparticles will be saturated with red light to induce an active conformation of PhyB to achieve steady state and then irradiated with far-red light to initiate disaggregation.

Characterize dark reversion-based disaggregation dynamics: Dark reversion-based disaggregation will be characterized by analyzing the influences of the conformational change of

PhyB from Pfr to Pr during transient and steady states. This experiment can be done during the end of characterizing the aggregation dynamics. Images of the colloidal suspensions will be taken during the steady state of aggregation and an absorbance measurement will be taken to quantify the dark reversion disaggregation kinetics.

Characterize irradiation pulse width for controlling aggregation: Red and far-red light will be pulsed intermittently to the colloidal suspensions to test the intermediate levels of aggregation. This will help maintain steady state conditions of the colloidal suspensions. Any patterns of pulse trains delivered to the suspensions, such as duty cycles and synchronization can be used to correlate with a given intermediate aggregation level. Therefore, tunable conditions could be established to transition between intermediate levels by adjusting the duty cycles of light pulses. Images and absorbance measurements will also be taken during these intermittent pulse waves to quantify and monitor the transient and steady states.

Image aggregate structures: Morphological images of the aggregated colloidal suspension will be taken using the same approach as in characterizing the aggregation dynamics. Examining the static and dynamic structures of these colloidal suspensions could be used as building blocks to create functional materials at the macroscopic level through programmable delivery of light signals. Mixtures of different sized nanoparticles at different concentration ratios can be used to create unique structures.

4. METHODS

PhyB and PIF3 Expression

Production of PhyB

All PhyB growth experiments were conducted in "dark room conditions". 100 mL of PhyB agar plates were prepared with a mixture of 1 g NaCl, 0.5 g yeast extract, 1 g bactone tryptone, and 1.5 g agar and autoclaved. Antibiotic final concentration of 17 ug/mL chloramphenicol, 25 ug/mL spectinomycin, 15 ug/mL kanamycin, and 1% glucose (17 C, 25 S, 15 K, 1 G) were added to plate media once cooled. PhyB plates were poured and stored at 4°C. PhyB plates were streaked from half antibiotic PhyB cell stock containing the final antibiotic concentration listed above and used within one week.

Media stock and preparation includes a 10:5:10 ratio for 1 L culture of 10 g NaCl, 5 g yeast extract, and 10 g bactone tryptone. Four 5 mL test tube cultures were prepared with the same antibiotic final concentration mixture (17 C, 25 S, 15 K, 1 G) and a single colony from the PhyB plate was added to each of the test tubes. The PhyB test tube cultures were incubated in a tabletop shaker incubator at 37°C and 225 rpm for 2.5 hours. Two 125 mL shake flask cultures were prepared with the antibiotic mixture (17 C, 25 S, 15 K, 1 G) and one 5 mL test tube was split to inoculate each shake flask. The shake flask cultures grew at 37°C and 225 rpm for 2.5 hours before introduced into the bioreactor system.

The bioreactor system (5L Sartorius Biostat A Plus) was sanitized and prepared the same day the PhyB plate was streaked due to length of preparation time. 5 L of media was placed into bioreactor system and the pH probe was calibrated before the entire vessel was placed into the autoclave. The dissolved oxygen (DO) probe was also placed into the vessel before autoclaving

but can be calibrated afterwards. Once the bioreactor culture cooled, the system parameters were set at 37°C, 225 rpm cascade at 40% DO for a maximum stir rate of 625 rpm, and pH of 7.8. The antibiotic mixture was then added to the bioreactor culture and then both 125 mL shaker flask cultures were added to the bioreactor system. A 1 mL sample was taken every hour to test the optical density of PhyB for induction purposes. Once the optical density OD_{600} reached 0.6 the bioreactor culture was cooled to 18°C with the assistance of a chiller set at 8°C. 0.1 mM IPTG was added to the bioreactor culture once the bioreactor culture reached 18°C (about 4 hours after the 125 mL culture was introduced to the bioreactor culture). The bioreactor was left to grow overnight (about 14 hours). The cells from the 5 L bioreactor culture were harvested by centrifugation using six 500 mL centrifuge bottles in a Beckman Coultier with parameters 4500 rpm, 30 minutes, 4°C, and rotor JA-10. The supernatant was discarded and more bioreactor culture was added to each of the six 500 mL centrifuge bottles until all the 5 L was collected. The six centrifuged bottles with the cell pellets were stored at -80°C until purification of PhyB.

Production of PIF3

All PIF3 cultures and plates were prepared same as PhyB cultures except for using final concentration of 100 or 200 ug/mL ampicillin antibiotic. A PIF3 plate was streaked using a PIF3 cell stock and incubated overnight at 37ºC. Four 5 mL test tube cultures were prepared with final concentration of 100 ug/mL ampicillin and a single colony from the PIF3 plate was added to each test tube culture to grow for 2.5 hours at 225 rpm. Four 500 mL shake flask cultures were prepared with final concentration of 200 ug/mL ampicillin and each were inoculated with one of the test tube cultures to grow at 37°C and 225 rpm for 3 hours. The temperature was reduced to 22°C and induced with 0.2 mM IPTG and continued to grow overnight. Cells from the 2 L culture were harvested by centrifugation using four 500 mL centrifuged bottles in a

Beckman Coultier centrifuge with parameters 4500 rpm, 30 minutes, 4°C, and rotor JA-10. The supernatant was discarded and more 2 L culture was added to its designated centrifuge bottle until all the 2 L cultures were collected. The four centrifuged bottles with the cell pellets were stored at -80°C until purification of PIF3.

Purification of PhyB and PIF3

Purification of each protein could be done separately, but PhyB was purified under "dark room conditions". The cell pellets from one 500 mL centrifuge bottle of PhyB and four 500 mL centrifuge bottles of PIF3 were purified each time. The cell pellet weight was recorded and then resuspended with 5 mL of 50 mM Tris buffer per gram of cell pellet, 0.1% Triton X-100, and 10 mM betamercaptoethanol. To lyse the cells, a final concentration of 1 mg/mL fresh lysozyme was added to each cell pellet and iced for 30 minutes. To complete the lysis and to shear the DNA to decrease the viscosity of the lysate, each suspension was then poured into 50 mL centrifuge tubes and sonicated using a sonication dismembrator (Fisher Scientific Model 100 Ultrasonic Dismembrator) on ice (to dissipate the heat produced) 4 times at power level 4 for 10 seconds with a one-minute intermittent period between sonication intervals. Each suspension was centrifuged for 30 minutes at 4°C and 17000 rpm to remove the cell debris and any solid materials to clarify the lysate.

A 3 mL Ni-NTA agarose column (Qiagen Ni-NTA Agarose beads) was equilibrated with six column bed volumes of 50 mM Tris buffer for each protein. The agarose column was drained to the top of the bed. The cell lysate for each protein was kept on ice after centrifugation and a 40 uL sample of the cell lysate was taken for SDS-PAGE analysis and 20 uL of 5X SDS-PAGE loading buffer was added to the sample. Each cell lysate was added to their respective

column and mixed with the column via transfer pipet to achieve optimal binding. Once the column settled, the cell lysate was allowed to flow through the column at a rate of 2 drops per second. The flow through was collected and a 40 uL sample was taken for SDS-PAGE analysis and added to 20 uL of 5X SDS-PAGE loading buffer. The column was then washed with 5 bed volumes of 25 mM imidazole and then a 40 uL sample of the 25 mM imidazole wash was collected and mixed with 20 uL of 5X SDS-PAGE loading buffer. The column was then washed with 4 bed volumes of 50 mM imidazole and a 40 uL sample of the 50 mM imidazole wash was collected and mixed with 20 uL of 5X SDS-PAGE loading buffer. One bed volume of 250 mM imidazole was added to the column and fractions were collected in three 1 mL microcentrifuge tubes. A 40 uL sample of each 250 mM imidazole fraction was collected and mixed with 20 uL of 5X SDS-PAGE loading buffer. One bed volume of 500 mM imidazole was added to the column and collected in three 1 mL microcentrifuge tubes. A 40 uL sample of each 500 mM imidazole fraction was collected and mixed with 20 uL of 5X SDS-PAGE loading buffer for SDS-PAGE analysis. The three 250 mM imidazole fractions were added to a PD-10 desalting column (GE Healthcare 17-0851-01 PD-10 Columns). The PD-10 column was equilibrated with 9 column loads (about 36 mL) before any protein was introduced to the column. The fractions were collected through the PD-10 column and then 100 uL aliquots were prepared in microcentrifuge tubes that were later flash frozen using liquid nitrogen. Purified protein aliquots were stored in -80°C freezer.

Characterization of recombinant PhyB in solution

Absorption spectra and difference spectra

All PhyB characterization experiments were conducted in "dark room conditions". The absorbance spectra and difference spectra were measured using a Molecular Devices 384 Spectra plus 96 well microplate reader, Reichert Scientific Instruments Model 1177 150 Watt output light source, and Semrock BrightLine 660/740 nm neutral filters. A volume of 400 uL 50 mM Tris buffer was added to well A1 for control and 400 uL 43.67 ug/mL purified PhyB protein was added to well A2. The samples were irradiated with far-red light at maximum light intensity of 0.885 mW using the 740 nm filter for 10 minutes. A spectral scan was conducted between 600 and 800 nm to achieve the inactive waveform for PhyB. The samples were then irradiated with red light at maximum light intensity of 1.664 mW using the 660 nm filter for 10 minutes to produce the active waveform. The data was imported into Microsoft excel to produce the difference spectra.

Light irradiance sensitivity

The PhyB protein was irradiated with different light intensities to help determine the amount of absorbed light by the protein while in suspension. The light source knob was labeled 1 through 5 and measured with a power meter (Ophir Starlite and PD300 photodiode sensor head with neutral density filter) to record the different light intensities for each filter wavelength as shown in Table 1.

Table 1. Reichert light source power level for 740 and 660 nm filter.

Pr form	740 nm filter	
Level	Wattage	Height
1	16.24 uW	1.27 cm
2	22.95 uW	
3	101.4 uW	
4	.286 mW	
5	.885 mW	

Pfr form	660 nm filter	
Level	Wattage	Height
1	23.08 uW	1.27 cm
2	31.3 uW	
3	155.6 uW	
4	.495 mW	
5	1.664 mW	

A spectral scan of the PhyB protein was taken for each filter wavelength at different light intensities and time intervals at a fixed distance from the Reichert light source. For example, one spectral scan of the Pr form of PhyB was irradiated at 16.24 uW of light for 30 seconds and at 1.27 cm away from the Reichert light source. The optical density at 662 nm was recorded from this Pr form scan to indicate the amount of light absorbed from the PhyB protein.

Dark reversion kinetics

The dark reversion kinetics were characterized by measuring the absorbance spectra as stated in 4.2.1. The PhyB sample was irradiated with far-red light/740 nm filter at intensity level 5 for 10 minutes and the optical density value at 720 nm was observed for analysis. The same procedure was used for red light conditions/660 nm filter. The optical density at 720 nm during red light irradiation was expected to be higher than far-red light irradiation so once this value was recorded an endpoint measurement at 720 nm for the PhyB sample was taken every 30 seconds to see how long it would take the PhyB sample to reach its inactive absorption spectra value at 720 nm for far-red light conditions.

Characterization of protein on polystyrene beads with counter protein in solution

Polystyrene bead preparation

A 1% (10 mg/mL) (100 uL of polystyrene beads in 900 uL of 50 mM Tris buffer) polystyrene bead solution was prepared from a 10% (100 mg/mL) polystyrene stock and diluted to a 0.1% (1 mg/mL) polystyrene solution. A 0.01% (0.1 mg/mL) polystyrene bead solution was then prepared and washed by centrifuging the solution with 1 mL of 50 mM Tris Buffer two times while replacing the supernatant between each centrifugation. The 0.01% polystyrene beads were finally resuspended with 1 mL of 1% F108-NTA and 50 mM Tris buffer solution and incubated by end-over-end mixing for 3 hours. The polystyrene/F108-NTA solution was charged with Ni^{2+} by incubating in 50 mM $NiSO_4$ with end-over-end mixing for 3 hours. The charged bead (CB) solution was centrifuged and then washed with 1 mL of 50 mM Tris Buffer to be stored in 4°C.

Immobilized PhyB with PIF3 in solution

Initial experiments contained a 1:1 ratio of immobilized protein to free protein in solution. Two Eppendorf tubes, labeled aggregated PhyB (AggB) and disaggregated PhyB (disAggB), were prepared with 50 uL of 44 ug/mL PhyB (Appendix A) mixed with 50 uL of 0.01% CB and incubated by end-over-end mixing for 1 hour. The two tubes of PhyB/CB mixture were centrifuged at 14000 rpm for 10 minutes in a tabletop centrifuge. The supernatant of each tube was collected and a 40 uL sample was mixed with 20 uL of 5X SDS-PAGE loading buffer to analyze free, unbound PhyB in solution. Each tube was then washed with 50 uL of 50 mM Tris buffer and centrifuged at 14000 rpm for 10 minutes to ensure all free, unbound PhyB was removed from solution. The supernatant of each tube was collected and a 40 uL sample was

mixed with 20 uL of 5X SDS-PAGE loading buffer for analysis. 50 uL of 44 ug/mL PIF3 (Appendix A) was added to each AggB and disAggB tube of the PhyB/CB mixture. The solutions were irradiated with far red light at intensity level 5 for 10 minutes. The disAggB tube was then centrifuged at 14000 rpm for 10 minutes. The supernatant of the disAggB tube was collected and a 40 uL sample was mixed with 20 uL of 5X SDS-PAGE loading buffer for analysis. The AggB tube was then irradiated with red light at intensity level 5 for 10 minutes. The AggB tube was centrifuged at 14000 rpm for 10 minutes. The supernatant of the AggB tube was collected and a 40 uL sample was mixed with 20 uL of 5X SDS-PAGE loading buffer for analysis.

Immobilized PIF3 with PhyB in solution

Initial experiments contained a 1:1 ratio of immobilized protein to protein in solution. Two Eppendorf tubes, labeled aggregated PIF3 (Agg3) and disaggregated PIF3 (disAgg3), were prepared with 50 uL of 44 ug/mL PIF3 mixed with 50 uL of 0.01% CB and incubated by end-over-end mixing for 1 hour. The two tubes of PIF3/CB mixture were centrifuged at 14000 rpm for 10 minutes. The supernatant of each tube was collected and a 40 uL sample was mixed with 20 uL of loading buffer for SDS-PAGE analysis to analyze free, unbound PIF3 in solution. Each tube was then washed with 50 uL of 50 mM Tris buffer and centrifuged at 14000 rpm for 10 minutes to ensure all free, unbound PIF3 was removed from solution. The supernatant of each tube was collected and a 40 uL sample was mixed with 20 uL of 5X SDS-PAGE loading buffer for analysis. 50 uL of PhyB was added to each Agg3 and disAgg3 tube of the PIF3/CB mixture. The solutions were irradiated with far red light at intensity level 5 for 10 minutes. The disAgg3 tube was then centrifuged at 14000 rpm for 10 minutes. The supernatant of the disAgg3 tube was collected and a 40 uL sample was mixed with 20 uL of 5X SDS-PAGE loading buffer for

analysis. The Agg3 tube was then irradiated with red light at intensity level 5 for 10 minutes. The Agg3 tube was centrifuged at 14000 rpm for 10 minutes. The supernatant of the Agg3 tube was collected and a 40 uL sample was mixed with 20 uL of 5X SDS-PAGE loading buffer for analysis.

Characterization of protein on magnetic beads with counter protein in solution

Magnetic agarose bead preparation

The magnetic beads were used in comparison with the polystyrene beads. These pre-charged agarose-coated magnetic particles possess NTA groups for chelating nickel which assist in the immobilization of his-tagged proteins for purification processes. With the convenience of their size and functionality, these magnetic beads make a great candidate for disaggregation and aggregation experiments. A 100 uL sample of 25% (v/v) magnetic beads was diluted with 400 uL of 50 mM Tris buffer to give an average settled magnetic beads solution of 25 uL. This 5% magnetics beads solution was centrifuged and washed with 500 uL of 50 mM Tris buffer twice to remove any residual storage buffer from the stock solution. Finally, the washed beads were stored at 4°C.

Immobilized PhyB with PIF3 in solution

Initial experiments contained a 1:1 ratio of immobilized protein to protein in solution. The procedure followed the same format as 4.3.2, but centrifugation was replaced with a magnetic Eppendorf stand.

Immobilized PIF3 with PhyB in solution

Initial experiments contained a 1:1 ratio of immobilized protein to protein in solution. The procedure followed the same format as 4.3.3, but centrifugation was replaced with a magnetic Eppendorf stand.

SDS-PAGE analysis

Ten 10% SDS-PAGE gels were cast at a time and stored in water-soaked paper towels and plastic wrap to avoid drying and stored at 4°C for preservation. A 10 uL sample from the SDS-PAGE samples stated in 4.1.3 were used to analyze protein purification and the samples in 4.3.2, 4.3.3 to analyze polystyrene bead characterization and 4.4.2, 4.4.3 to analyze magnetic bead characterization. Rockland Molecular Weight marker was used as reference for protein weight. The electrophoresis ran for 1.5 hours at 130 volts. Coomassie staining and destaining procedure was completed as stated in Appendix B.

Protein concentration assay

Protein concentration was measured using the Bradford Assay at 595 nm (Lambda 45 Spectrophotometer) with a BSA standard. BSA standard curve was created by measuring the optical density for known concentrations of 0.04, 0.032, 0.024, 0.016, and 0.008 mg/mL BSA mixed with 50 mM Tris buffer at a total volume of 500 uL. 500 uL of Bradford Assay was added to each BSA concentration and allowed to sit for 10 minutes. Protein concentration curves for PhyB and PIF3 were created by measuring the optical density for each protein at dilution factors of 0.2, 0.15, 0.1, and 0.05 mixed with 50 mM Tris buffer at a total volume of 500 uL. 500 uL of Bradford Assay was added to each protein dilution factor and allowed to sit for 10 minutes.

Depletion assay

The depletion assay procedure used the same format as in 4.3 and 4.4. Each supernatant sample was mixed with 50 mM Tris buffer to a final volume of 500 uL and then 500 uL of Bradford Assay was added to let stand for 10 minutes. Protein concentration was measured at 595 nm using Lambda 45 Spectrophotometer with a BSA standard.

Polystyrene and magnetic bead imaging

Imaging of the beads was conducted using an EVOS microscope. Polystyrene bead images were taken with samples in glass depression slides at 40X magnification and magnetic bead images were taken with samples in a microplate at 10X and 4X magnification. Samples were prepared as follows:

Polystyrene Beads

Sample 1. 50 uL of 0.01% polystyrene beads with 50 uL of 50 mM Tris buffer

Sample 2. 50 uL of 43.67 ug/mL PhyB on 50 uL of 0.01% polystyrene beads

Sample 3. 50 uL of 44.42 ug/mL PIF3 on 50 uL of 0.01% polystyrene beads

Sample 4. 50 uL of 43.67 ug/mL PhyB on 50 uL of 0.01% polystyrene beads mixed with 50 uL of 44.42 ug/mL PIF3 on 50 uL of 0.01% polystyrene beads

Magnetic Beads

Well A1. 10 uL of magnetic beads with 100 uL of 50 mM Tris buffer

Well A2. 50 uL of 43.67 ug/mL PhyB on 10 uL of magnetic beads and 50 uL of 50 mM Tris buffer

Well B1. 50 uL of 44.42 ug/mL PIF3 on 10 uL magnetic beads with 50 uL of 50 mM Tris buffer

Well B2. 50 uL of 43.67 ug/mL PhyB on 10 uL of magnetic beads mixed with 50 uL of 44.42 ug/mL PIF3 on 10 uL of magnetic beads

CHAPTER 5: RESULTS

Protein Expression

PhyB

PhyB expression was achieved by using a 5 L bioreactor to produce greater quantities to perform these experiments for this project. Initial SDS-PAGE experiments were conducted to show which imidazole fraction released the purest protein from the column. The SDS-PAGE gels as seen in Figure 8 depict the chromatographic fractions to produce the purified PhyB. Lanes 2 and 3 in Figure 8a show the clarified lysate added to the IMAC column and the flow through from the column, respectively. Lanes 4 – 8 in Figure 8a display the wash used for removing contaminants and the imidazole fractions used to elute any weakly bound proteins and the PhyB protein of interest from the IMAC media. Purified PhyB was taken from lanes 5, 6, and 7 in Figure 8b as these fractions were estimated to be around 75% pure. The 500 mM imidazole fractions were included to show the clearance of any remaining PhyB on the column that may have been missed with dilute solutions of imidazole. Therefore, for subsequent chromatography experiments all PhyB protein was washed with 5 bed volumes of 25 mM imidazole, 4 bed volumes of 50 mM imidazole, and purified from the last three 250 mM imidazole fractions.

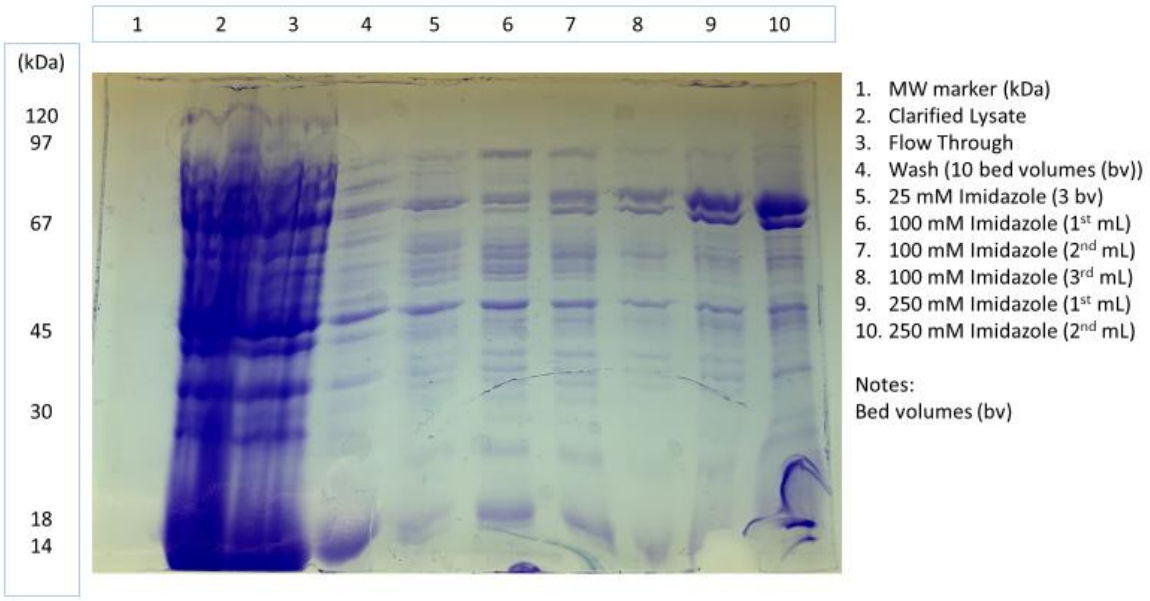

(a).

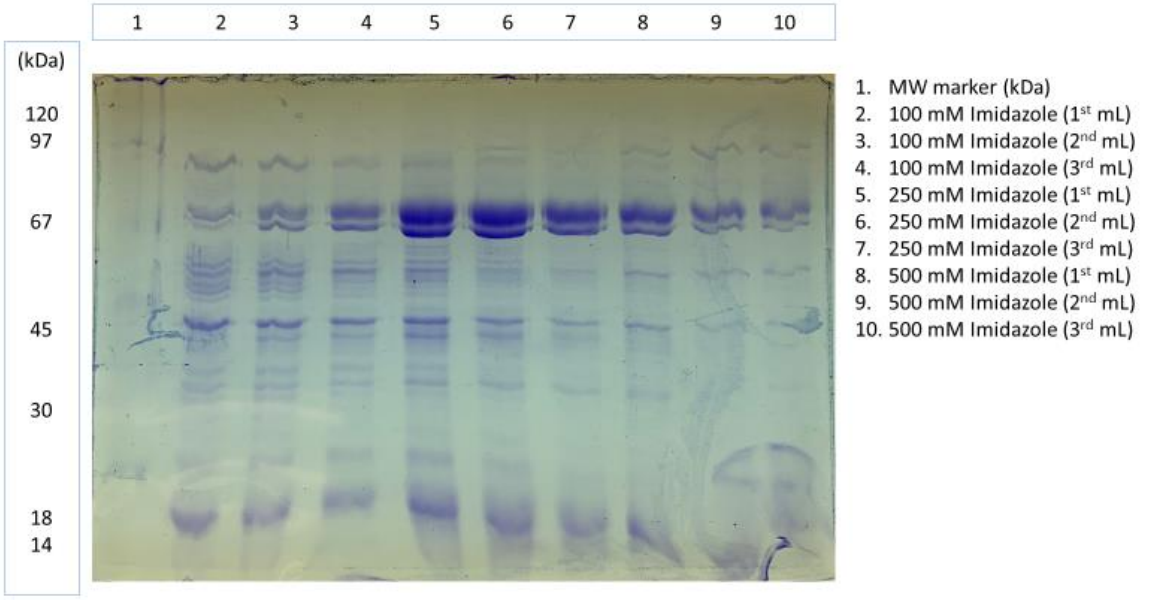

(b).

Figure 8. SDS-PAGE analysis of PhyB IMAC purification. Two gels were used to analyze all the samples from the same purification run. Majority of PhyB was eluted from the 250 mM imidazole fractions and clearance from the column was from the 500 mM imidazole fractions.

PIF3

PIF3 expression was achieved by using four 500 mL shake flask cultures to produce enough protein to perform the experiments for this project. Initial SDS-PAGE experiments were conducted to determine which imidazole fraction released the purest protein from the column. The SDS-PAGE gels shown in Figure 9 depict the chromatographic fractions of the IMAC purification process for PIF3. Lanes 2 and 3 showed the clarified lysate added to the IMAC column and flow through from the column, respectively. Lanes 4 and 5 in Figure 9a display the 25 and 50 mM imidazole washes used for removing contaminants and elute any weakly bound proteins from the IMAC media. Purified PIF3 was taken from lanes 7, 8, and 9 in Figure 9a as these fractions were the purest samples. The 500 mM imidazole fractions were included to show the clearance of any remaining PIF3 on the column that may have been missed with dilute solutions of imidazole. Therefore, for subsequent chromatography experiments all PIF3 protein was washed with 5 bed volumes of 25 mM imidazole, 4 bed volumes of 50 mM imidazole, and purified from the last three 250 mM imidazole fractions.

Characterization of recombinant PhyB in solution

Absorption spectra and difference spectra

The absorbance spectra for the Pr and Pfr form of PhyB are shown in Figure 10. The PhyB sample was first irradiated with light at 740 nm for 10 minutes at the maximum light intensity of 0.885 mW to transform the protein into its inactive conform. This produced the Pr waveform with the highest peak detected at 662 nm. The PhyB sample was then irradiated with light at 660 nm for 10 minutes at maximum light intensity of 1.664 mW to transform the protein into its active conform. This produced the Pfr waveform with peak detection at 670 and 724 nm.

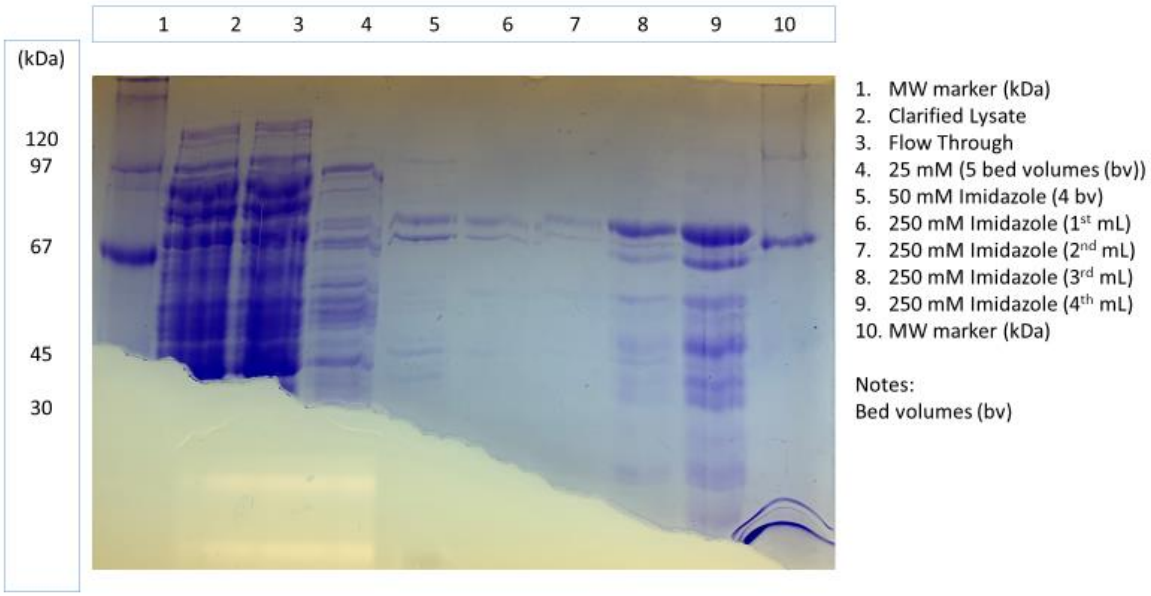

(a).

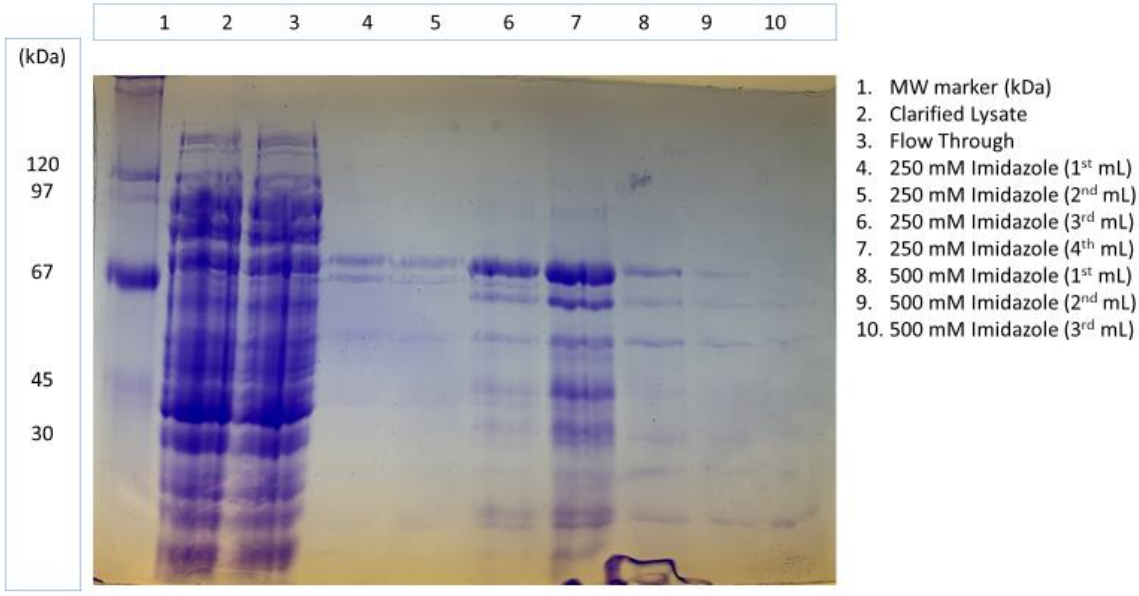

(b).

Figure 9. SDS-PAGE analysis of PIF3 IMAC purification. Two gels were used to analyze all the samples from the same purification run. Majority of PIF3 was eluted from the 250 mM imidazole fractions and clearance from the column was from the 500 mM imidazole fractions.

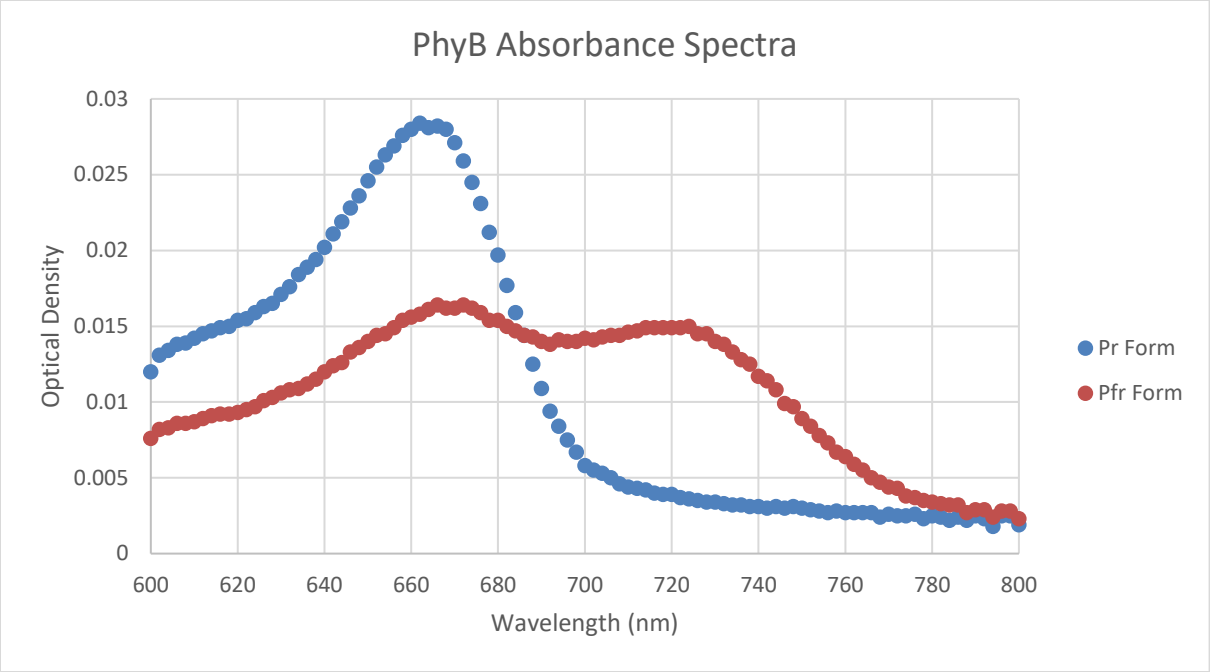

Figure 10. Absorption spectra of Pr and Pfr form of PhyB. The PhyB protein absorbs far-red light at a peak of 662 nm and absorbs red light at peaks of 670 nm and 724 nm.

A difference spectra was taken to confirm the PhyB protein does transition between its inactive and active form upon its respective light irradiation wavelength shown in Figure 11. This difference spectra was produced by subtracting the Pfr data from the Pr data to illustrate the wavelengths at which the PhyB protein absorbs light for its inactive and active form. Therefore, the PhyB absorbs far-red light at 662 nm and red light at 724 nm.

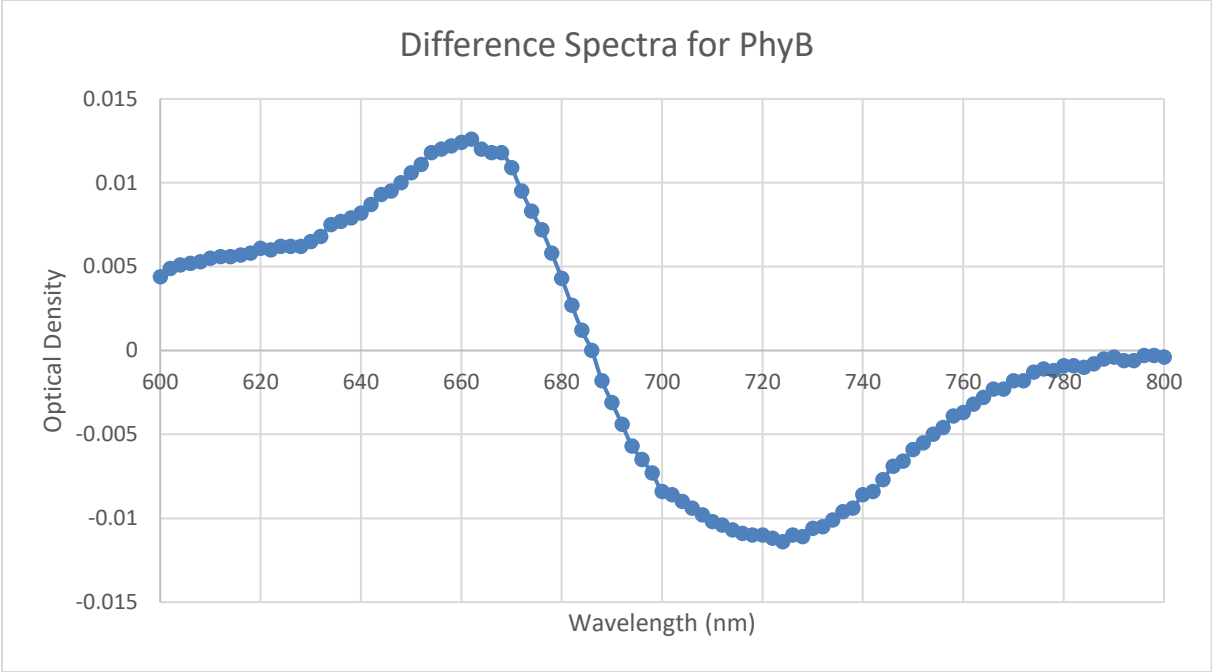

Figure 11. Difference spectra for PhyB. This difference spectra was generated by taking the difference of the Pfr data from the Pr data in Figure 6 to illustrate the peak detection of PhyB when irradiated with far-red and red light. Peaks were recorded for far-red and red light irradiation at 662 and 724 nm respectively.

Light irradiance sensitivity

A spectral scan of PhyB was created for the Pr and Pfr form for the different light intensities at various time intervals. The first comparison of spectral scans was light intensity at a set time interval of 10 minutes. As shown in Figures 12 and 13, the optical density was directly proportional to light intensity as more PhyB absorbed at a higher intensity of light. The same relationship was observed as the PhyB protein was irradiated with a fixed light intensity, but at different time intervals. As shown in Figures 12 and 14, the optical density was proportional to the amount of time the PhyB was irradiated at a fixed light intensity. Each optical density was recorded in Table 2, which indicated that more PhyB will be absorbed at a longer duration at maximum light intensity. The optical density values were converted to the

amount of PhyB absorbed in nmol to indicate how much PhyB was active at each light intensity level and duration of irradiation.

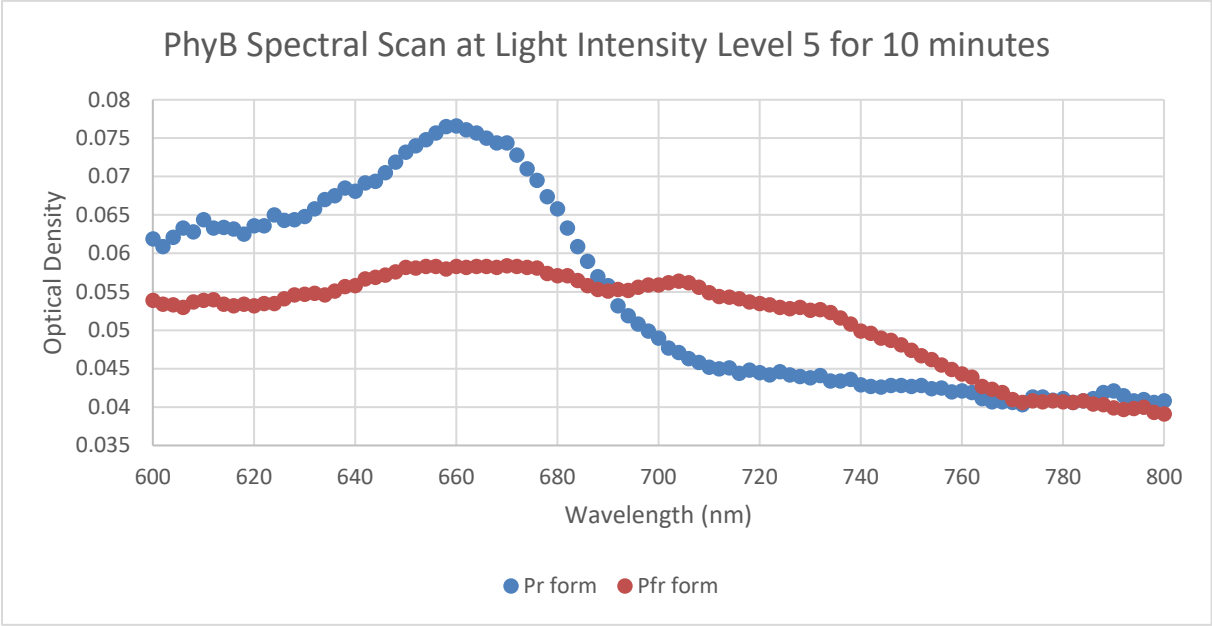

Figure 12. Absorption spectra for PhyB at Light Intensity Level 5 for 10 minutes. PhyB protein was irradiated with the 740 nm filter at 0.885 mW for 10 minutes to produce the Pr spectra and with the 660 nm filter at 1.664 mW for 10 minutes to produce the Pfr spectra.

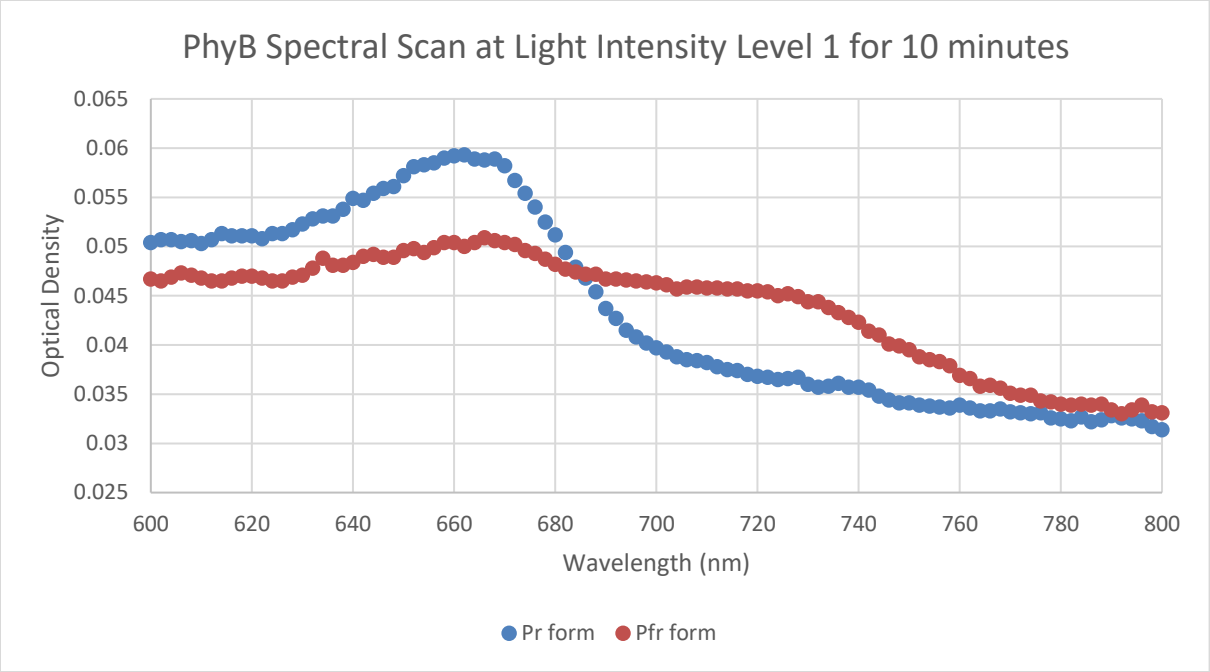

Figure 13. Absorption spectra for PhyB at Light Intensity Level 1 for 10 minutes. PhyB protein was irradiated with the 740 nm filter at 16.24 uW for 10 minutes to produce the Pr spectra and with the 660 nm filter at 23.08 uW for 10 minutes to produce the Pfr spectra.

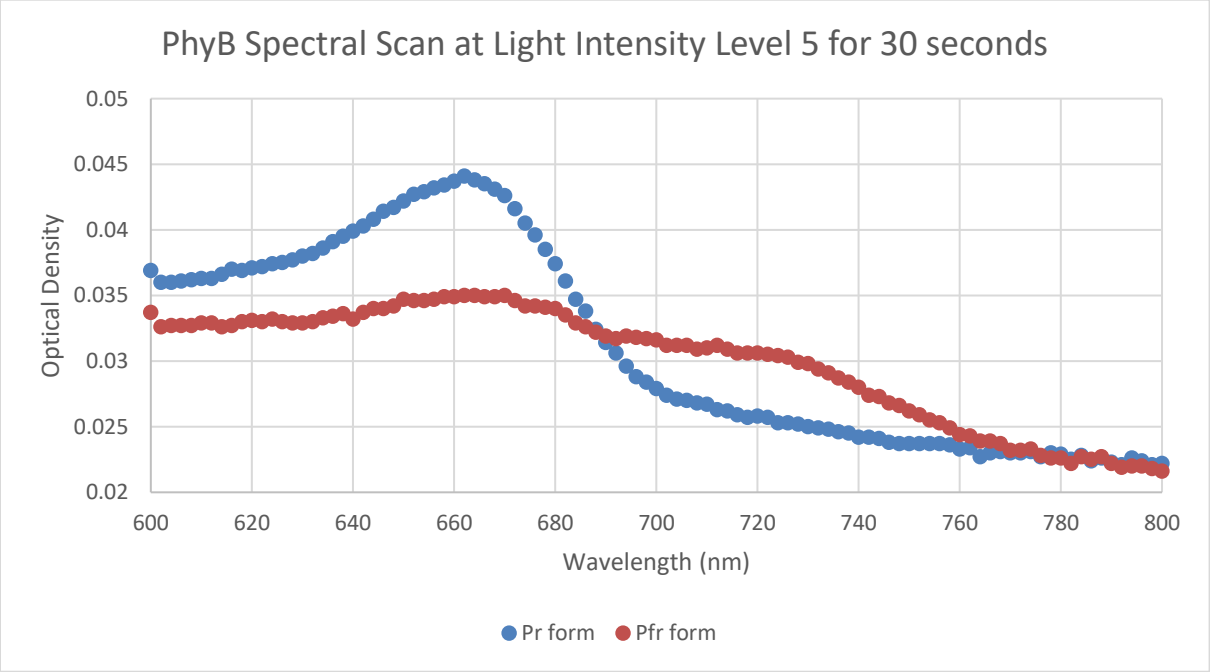

Figure 14. Absorption spectra for PhyB at Light Intensity Level 5 for 30 seconds. PhyB protein was irradiated with the 740 nm filter at 0.885 mW for 30 seconds to produce the Pr spectra and with the 660 nm filter at 1.664 mW for 30 seconds to produce the Pfr spectra.

Table 2. Light Irradiance Sensitivity Data

Pr form (Absorbance)						
		Light Intensity Level				
		1 (16.24 uW)	2 (22.95 uW)	3 (101.4 uW)	4 (0.286 mW)	5 (0.885 mW)
Time	30 s	0.0364	0.0361	0.0407	0.0422	0.0441
	1 min	0.0391	0.0413	0.0438	0.0456	0.047
	2 min	0.0425	0.0425	0.0473	0.0502	0.0526
	5 min	0.0493	0.0563	0.0505	0.0596	0.061
	10 min	0.0593	0.0631	0.0642	0.0635	0.0761
		Absorbance				
Wavelength Measured - 662 nm						

Pr form (nmol of PhyB absorbed)						
		Light Intensity Level				
		1 (16.24 uW)	2 (22.95 uW)	3 (101.4 uW)	4 (0.286 mW)	5 (0.885 mW)
Time	30 s	0.1160	0.1151	0.1298	0.1345	0.1406
	1 min	0.1247	0.1317	0.1396	0.1454	0.1498
	2 min	0.1355	0.1355	0.1508	0.1600	0.1677
	5 min	0.1572	0.1795	0.1610	0.1900	0.1945
	10 min	0.1891	0.2012	0.2047	0.2024	0.2426
		nmol of PhyB absorbed				
Wavelength Measured - 662 nm						

Pfr form						
		Light Intensity Level				
		1 (23.08 uW)	2 (31.3 uW)	3 (155.6 uW)	4 (0.495 mW)	5 (1.664 mW)
Time	30 s	0.0283	0.0289	0.0291	0.0308	0.0304
	1 min	0.0317	0.0317	0.0322	0.0329	0.0322
	2 min	0.0319	0.0339	0.0331	0.0347	0.035
	5 min	0.0361	0.036	0.0366	0.0419	0.0427
	10 min	0.045	0.0458	0.048	0.0463	0.053
		Absorbance				
Wavelength Measured - 724 nm						

Pfr form (nmol of PhyB Absorbed)						
		Light Intensity Level				
		1 (23.08 uW)	2 (31.3 uW)	3 (155.6 uW)	4 (0.495 mW)	5 (1.664 mW)
Time	30 s	0.1295	0.1323	0.1332	0.1410	0.1392
	1 min	0.1451	0.1451	0.1474	0.1506	0.1474
	2 min	0.1460	0.1552	0.1515	0.1588	0.1602
	5 min	0.1653	0.1648	0.1675	0.1918	0.1955
	10 min	0.2060	0.2097	0.2197	0.2119	0.2426
		nmol of PhyB absorbed				
Wavelength Measured - 724 nm						

Dark reversion kinetics

The dark reversion kinetics of PhyB were analyzed by first irradiating the PhyB protein with far-red light for 10 minutes to ensure all protein was in its inactive conformation and measuring the optical density at 720 nm to measure the baseline absorbance value. Then the protein was saturated with red light for 10 minutes and the optical density was measured at 720 nm until it reached the baseline optical density for far-red light conditions. The optical density value at 720 nm for far-red light conditions was 0.0165 and for red light conditions was 0.0295. According to Figure 15, the PhyB protein naturally reverted to its Pr form in around 5 hours. The optical density data was converted to the amount of PhyB absorbed to obtain the relationship

of how much PhyB had reverted over the 5 hour period.

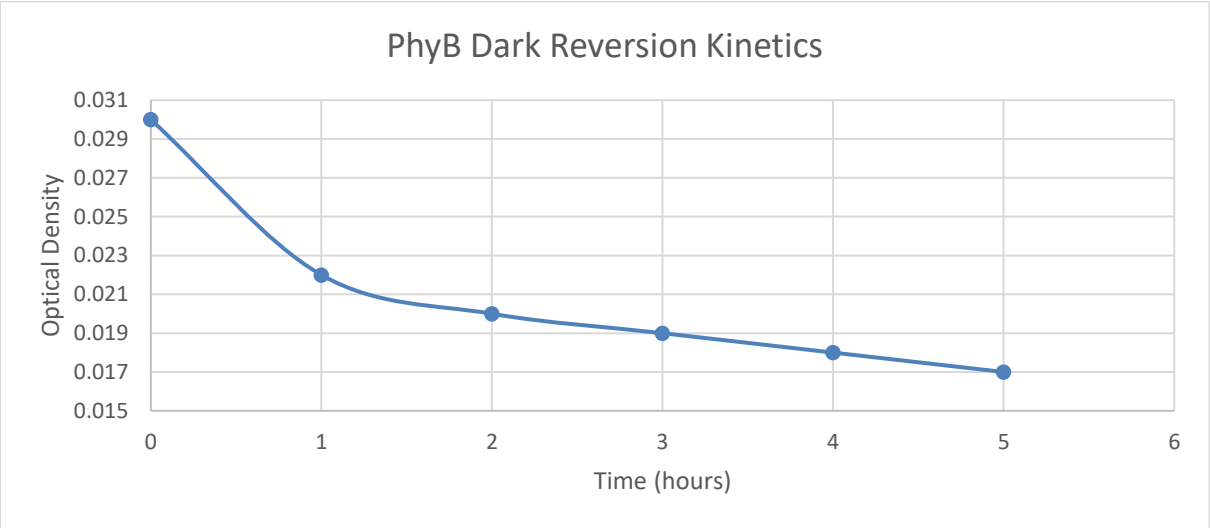

(a).

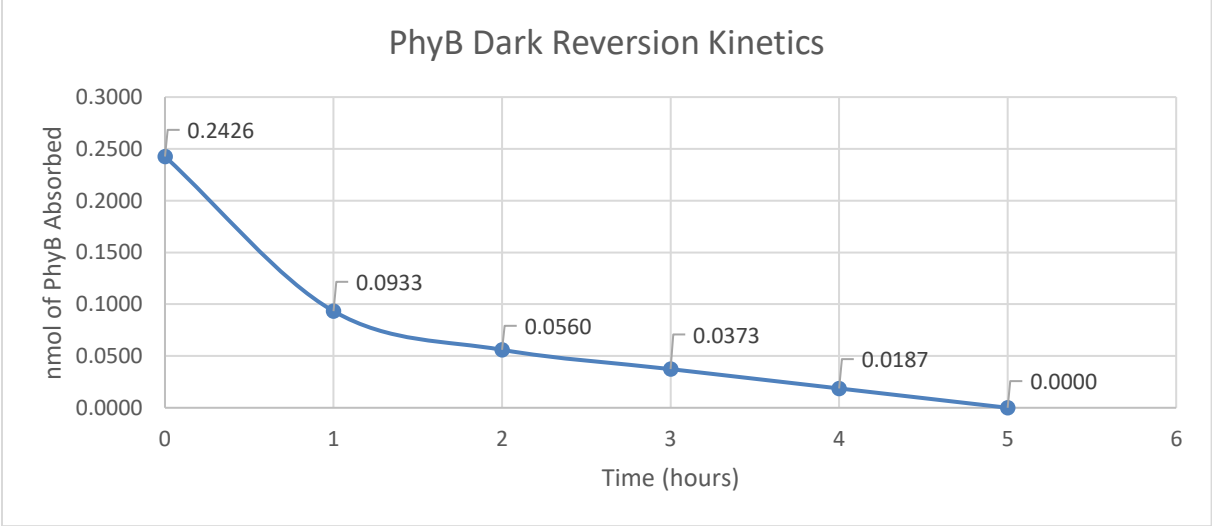

(b).

Figure 15. Dark Reversion Kinetics for PhyB. (a). The PhyB protein naturally reverted to its inactive form by observing the optical density at 720 nm for far-red and red light conditions. An optical density reading of 0.0165 and 0.0295 at 720 nm was recorded under far-red and red light conditions, respectively. (b). The optical density for each data point was converted to nmol of PhyB absorbed to get a relative amount of protein reverted to its inactive form over time.

Characterization of protein on beads with counterpart protein in solution

Immobilization of PhyB and PIF3 on polystyrene beads

Results from initial experiments to immobilize PhyB and PIF3 to a 0.1% (1 mg/mL) polystyrene bead solution using SDS-PAGE analyses is shown in Figure 16. Lane 1 represents the molecular weight marker in kDa. A sample of untreated 0.1% polystyrene beads was loaded into lane 2 and as expected no bands were present. Lane 3 was 40 uL of 44 ug/mL of PhyB in solution which was used as a reference. Lane 4 represented the amount of PhyB left in solution after centrifuging the one-hour end-over-end mixture of 50 uL of 44 ug/mL PhyB protein and 50 uL of 0.1% polystyrene beads. Lane 5 shows the amount of PhyB protein left on the beads after being treated with 20 uL of 5X SDS-PAGE loading buffer to strip the protein off the bead surface. Lanes 6, 7, and 8 are the same samples as lanes 3, 4, and 5 except with PIF3 as the protein of interest. Lanes 5 and 8 in Figure 16 illustrate both PhyB and PIF3, respectively, were immobilized on the 0.1% polystyrene beads with little or no PhyB and PIF3 left in solution in lanes 4 and 7, respectively. As a result of these proteins immobilizing on 0.1% plolystyrene beads, the next set of experiments used 0.01% polystyrene beads to characterize the immobilization of one protein on the surface with the other protein in solution.

Characterization of protein on 0.01% polystyrene beads with counterpart protein in solution

The next step was to analyze the interactions between proteins when one was immobilized on 0.01% polystyrene beads with the counterpart protein in solution. As shown in Figure 17, lane 5 to 8 and 6 to 9 were compared for unbound protein during far-red light irradiation and bound protein for red light irradiation. It is noted that lanes 6 and 9 cannot be

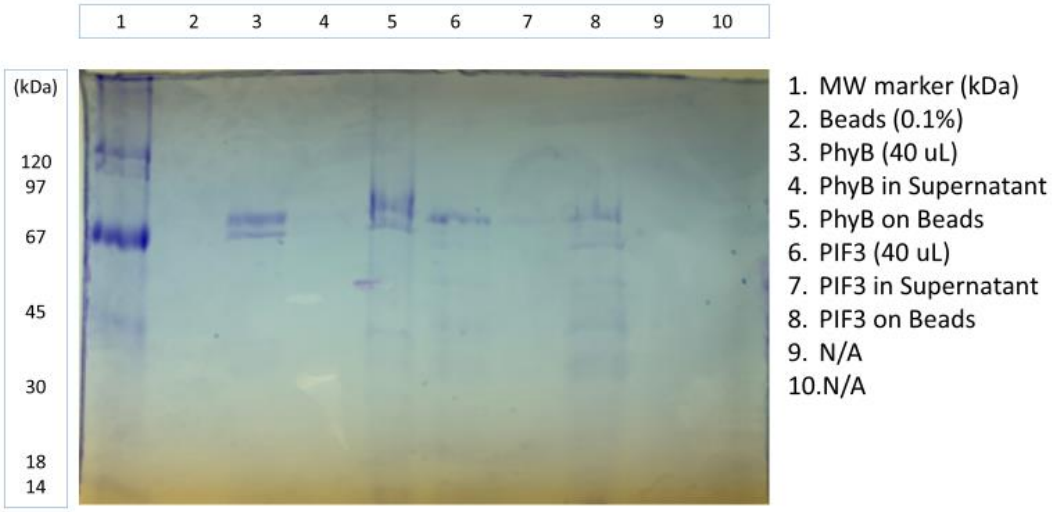

Figure 16. SDS-PAGE analysis PhyB and PIF3 immobilized on 0.1% polystyrene beads. Immobilization of PhyB and PIF3 on 0.1% polystyrene beads was achieved as seen in lanes 5 and 8, respectively.

compared qualitatively due to the similar molecular weights of both proteins. Comparing lane 5 to 8 for Figure 17.a, it is apparent when PIF3 was added to an immobilized PhyB that PIF3 remained in solution whether PhyB was inactive or active. This result is also seen in the Figure 17.b, however lane 5 seems to have a more prominent band of PhyB in solution than in lane 8 indicating the potential of active PhyB binding to an immobilized PIF3. However, these results were inconsistent with subsequent experiments which led to the use of magnetic beads for qualitative analysis.

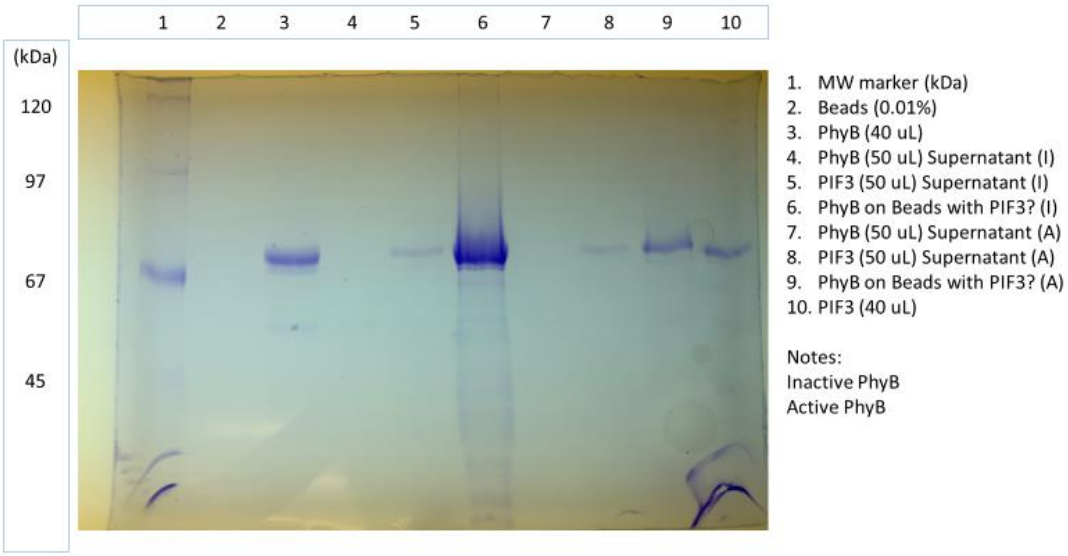
1 2 3 4 5 6 7 8 9 10
(kDa)
120
97
67
45
1. MW marker (kDa)
2. Beads (0.01%)
3. PhyB (40 uL)
4. PhyB (50 uL) Supernatant (I)
5. PIF3 (50 uL) Supernatant (I)
6. PhyB on Beads with PIF3? (I)
7. PhyB (50 uL) Supernatant (A)
8. PIF3 (50 uL) Supernatant (A)
9. PhyB on Beads with PIF3? (A)
10. PIF3 (40 uL)
Notes:
Inactive PhyB
Active PhyB

(a).

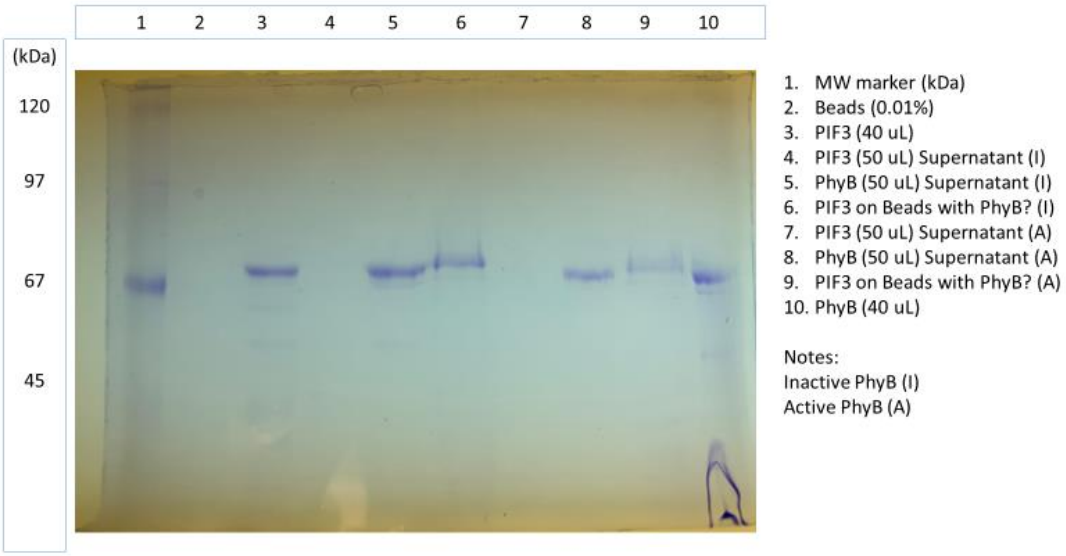

(b).

Figure 17. SDS-PAGE analysis of immobilized protein on 0.01% polystyrene beads with the counterpart protein in solution. (a). PhyB immobilized on polystyrene beads with PIF3 in solution. (b). PIF3 immobilized on polystyrene beads with PhyB in solution. Lane 1 – Molecular weight marker. Lane 2 – 0.01% polystyrene beads. Lane 3. 40 uL (43.67 ug/mL PhyB or 44.42 ug/mL PIF3) of reference protein. Lane 4 and 7 – Amount of protein referenced to lane 1 not immobilized. Lane 5 and 8 – Amount of protein in solution referenced to lane 10 after irradiation of far-red and red light respectively. Lane 6 and 9 – Amount of protein immobilized on polystyrene beads after irradiation of far-red and red light respectively. Lane 10. 40 uL (44.42 ug/mL PIF3 or 43.67 ug/mL PhyB) of reference protein.

Characterization of protein on 5% magnetic beads with counterpart protein in solution

SDS-PAGE analysis with the magnetic beads initially showed promising results with both proteins immobilized to the surface having the opposite protein in solution as seen in Figure 18. Like Figure 17.b, lane 9 compared to lane 5 suggests there was possible binding of the protein in solution to the immobilized protein. However, subsequent SDS-PAGE experiments did not replicate these results. Therefore, a depletion assay was conducted for each lane to quantify the protein content.

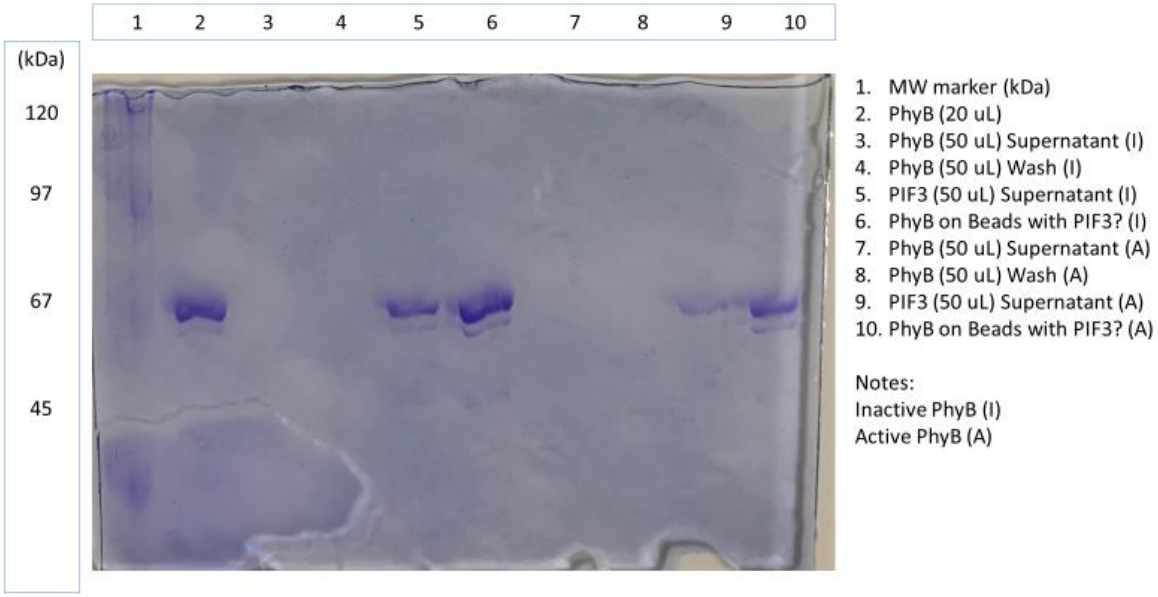
1 2 3 4 5 6 7 8 9 10
(kDa)
120
97
67
45
1. MW marker (kDa)
2. PhyB (20 uL)
3. PhyB (50 uL) Supernatant (I)
4. PhyB (50 uL) Wash (I)
5. PIF3 (50 uL) Supernatant (I)
6. PhyB on Beads with PIF3? (I)
7. PhyB (50 uL) Supernatant (A)
8. PhyB (50 uL) Wash (A)
9. PIF3 (50 uL) Supernatant (A)
10. PhyB on Beads with PIF3? (A)
Notes:
Inactive PhyB (I)
Active PhyB (A)

(a).

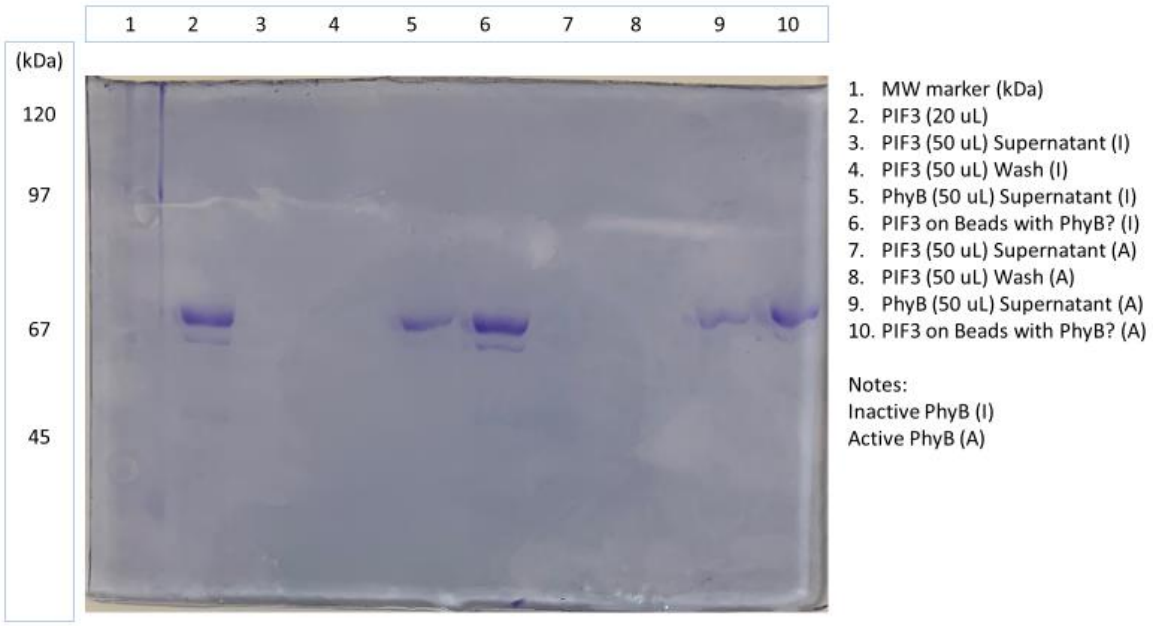

(b).

Figure 18. SDS-PAGE analysis of immobilized protein on magnetic beads with counterpart protein in solution. (a). PhyB immobilized on magnetic beads with PIF3 in solution. (b). PIF3 immobilized on magnetic beads with PhyB in solution. Inactive (I) and active (A) PhyB represent the samples contained the Pr and Pfr form of PhyB, respectively. Lane 1 – Molecular weight marker. Lane 2 – 20 uL (43.67 ug/mL PhyB or 44.42 ug/mL PIF3) of protein as reference. Lane 3 and 7 – Amount of protein referenced to lane 2 not immobilized. Lane 4 and 8 – Residual protein after magnetic bead wash. Lane 5 and 9 – Amount of protein in solution referenced to lane 2 after irradiation of far-red and red light respectively. Lane 6 and 10 – Amount of protein immobilized on magnetic beads after irradiation of far-red and red light respectively.

Depletion assay

Polystyrene beads

The depletion assay for polystyrene beads did not give any indication of the counterpart protein in solution binding to the immobilized protein on the bead surface when comparing lane 9 to 5 in Figure 19. The only comparable lanes between Figure 19.a and 19.b was how much protein bound to the surface of the polystyrene beads. With the addition of 50 uL of 44 ug/mL

PhyB to the polystyrene beads, about 60.1% were immobilized while only 46.4% of 50 uL of 44 ug/mL PIF3 was immobilized on the surface. Without quantifiable evidence for bound counter protein to immobilized protein with polystyrene beads, the depletion assay was also conducted using magnetic beads.

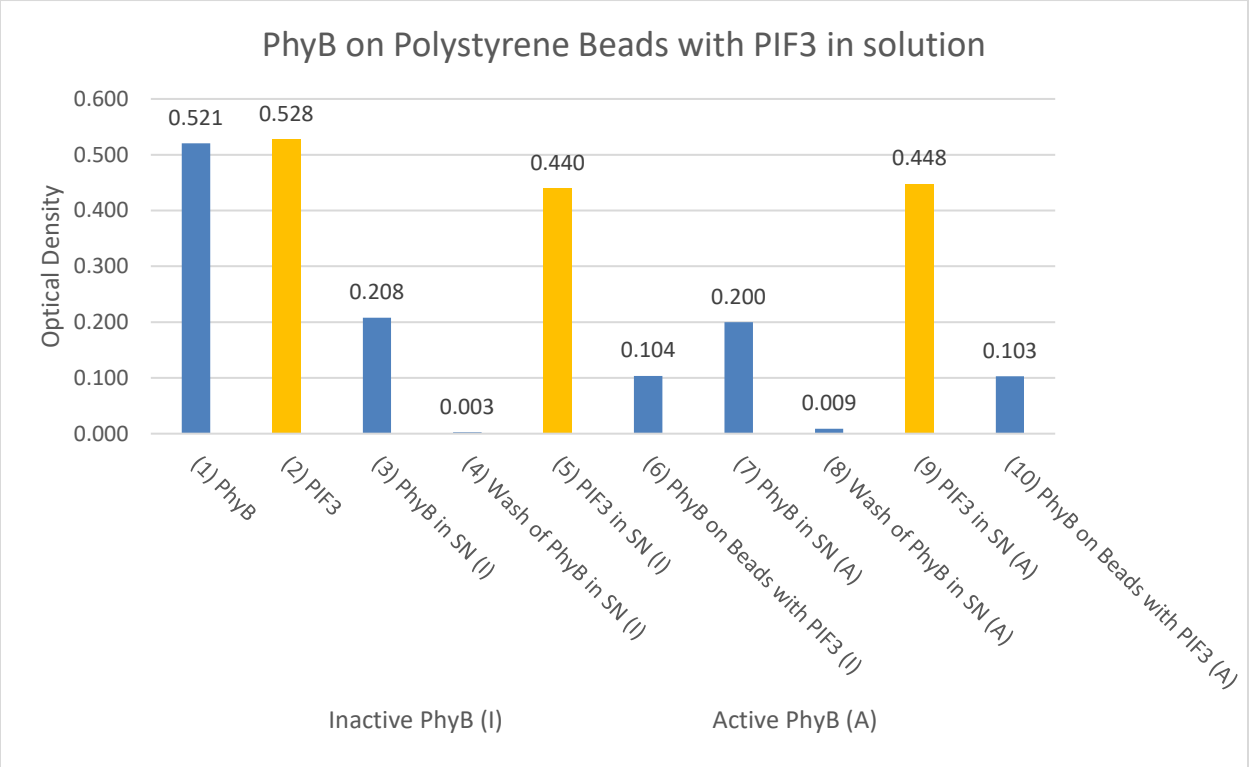

(a).

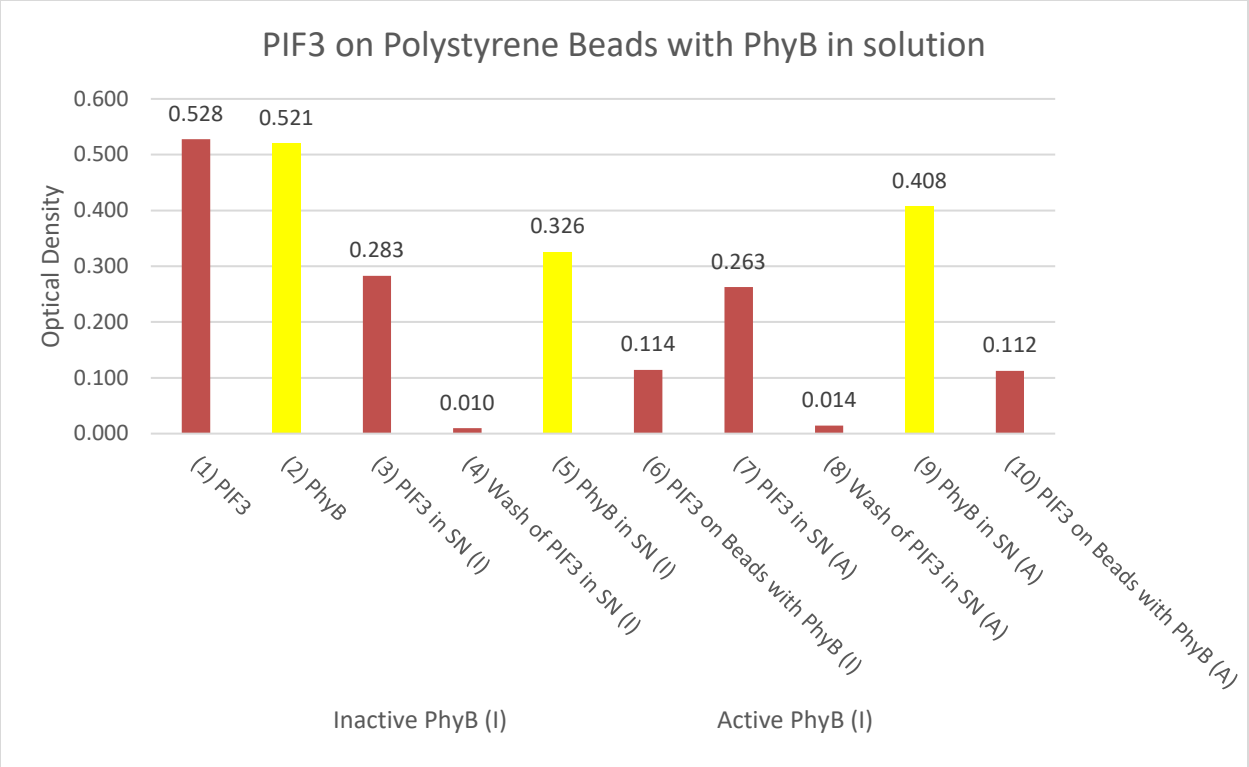

(b).

Figure 19. Depletion assay for 1:1 ratio of PhyB:PIF3 with Polystyrene Beads. (a). 50 uL of 43.67 ug/mL PhyB immobilized on 0.01% polystyrene beads with 50 uL of 44.42 ug/mL PIF3 in solution. (b). 50 uL of 44.42 ug/mL PIF3 immobilized on 0.01% polystyrene beads with 50 uL of 43.67 ug/mL PhyB in solution. Inactive (I) and active (A) PhyB represent the samples contained the Pr and Pfr form of PhyB, respectively. Lane 1 – 50 uL of protein added to polystyrene beads. Lane 2 – 50 uL of protein in solution. Lane 3 and 7 – Amount of protein referenced to lane 1 not immobilized. Lane 4 and 8 – Residual protein after polystyrene bead wash. Lane 5 and 9 – Amount of protein in solution referenced to lane 2 after irradiation of far-red and red light respectively. Lane 6 and 10 – Amount of protein immobilized on polystyrene beads after irradiation of far-red and red light respectively.

Magnetic beads

Even though the qualitative results for SDS-PAGE analysis using magnetic beads was difficult to replicate, the depletion assay produced a consistent trend when considering the counter protein in solution once added to immobilized protein after irradiated with far-red and red light. As seen in Figure 20, lane 9 showed a decrease of counter protein in solution

compared to lane 5 for both assays suggesting binding may have occurred during red light irradiation. It is also noted that about 61.1% of the 50 uL of 43.67 ug/mL PhyB and 71.9% 50 uL of 44.42 ug/mL PIF3 was immobilized to the magnetic bead surface as compared to immobilization of PhyB and PIF3 on polystyrene beads. Subsequent depletion assay experiments contained the same trend of less protein content in lane 9 as compared to lane 5 as shown in Appendix C.

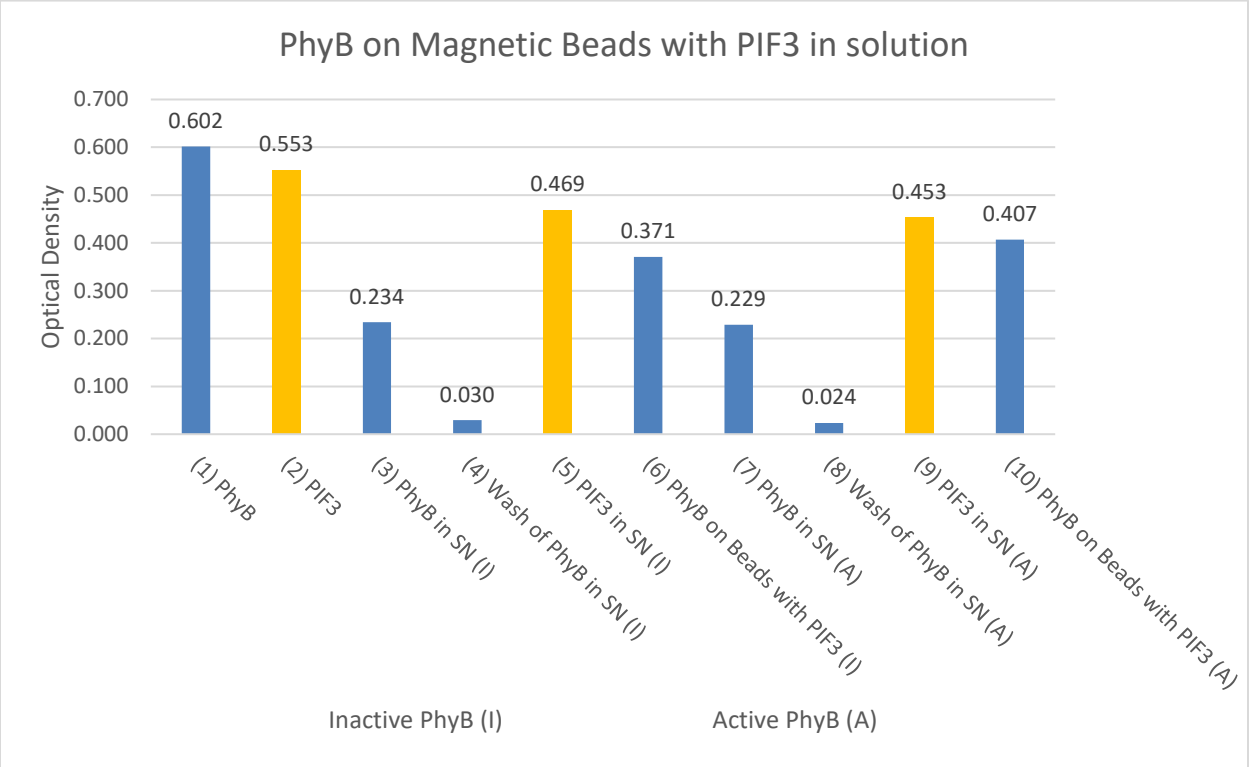

(a).

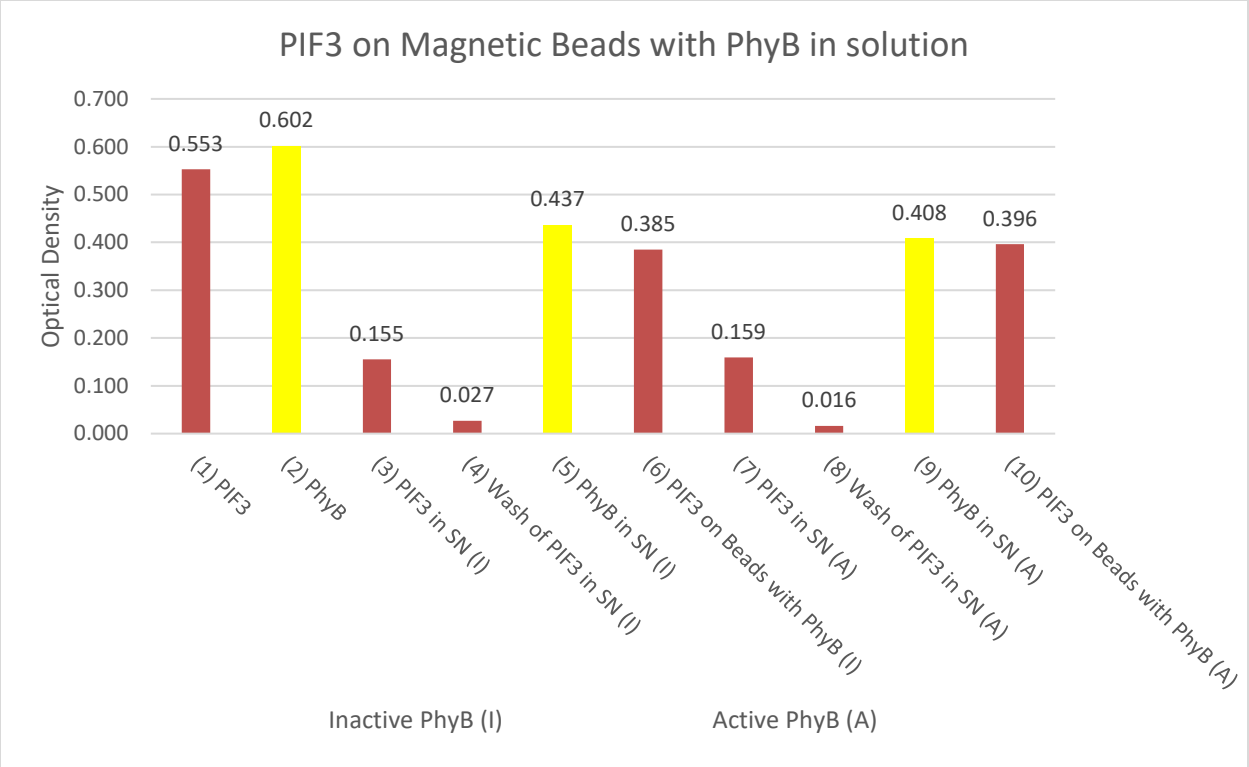

(b).

Figure 20. Depletion assay for 1:1 ratio of PhyB:PIF3 with Magnetic Beads. (a). 50 uL of 43.67 ug/mL PhyB immobilized on 10 uL of 5% magnetic beads with 50 uL of 44.42 ug/mL PIF3 in solution. (b). 50 uL of 44.42 ug/mL PIF3 immobilized on 10 uL of 5% magnetic beads with PhyB in solution. Inactive (I) and active (A) PhyB represent the samples contained the Pr and Pfr form of PhyB, respectively. Lane 1 – 50 uL of protein added to magnetic beads. Lane 2 – 50 uL of protein in solution. Lane 3 and 7 – Amount of protein referenced to lane 1 not immobilized. Lane 4 and 8 – Residual protein after magnetic bead wash. Lane 5 and 9 – Amount of protein in solution referenced to lane 2 after irradiation of far-red and red light respectively. Lane 6 and 10 – Amount of protein immobilized on magnetic beads after irradiation of far-red and red light respectively.

Imaging bead aggregation structures

Polystyrene beads

Based upon the initial SDS-PAGE analysis of light-induced binding with one protein immobilized and the other in solution, images of 0.01% polystyrene beads were taken with each protein immobilized on its own separate bead solution. One set of images has a mixture of PhyB

beads and PIF3 beads to capture if any aggregation occurs under red light conditions. As shown in Figure 21, there is inconclusive evidence of PhyB bead and PIF3 bead light-induced aggregation. An image of only polystyrene beads under far-red and red light irradiation was also taken as a reference shown in Appendix D. Therefore, magnetic NTA-Ni^{2+} agarose beads were used to compare surface immobilization for each protein and light-induced binding and unbinding.

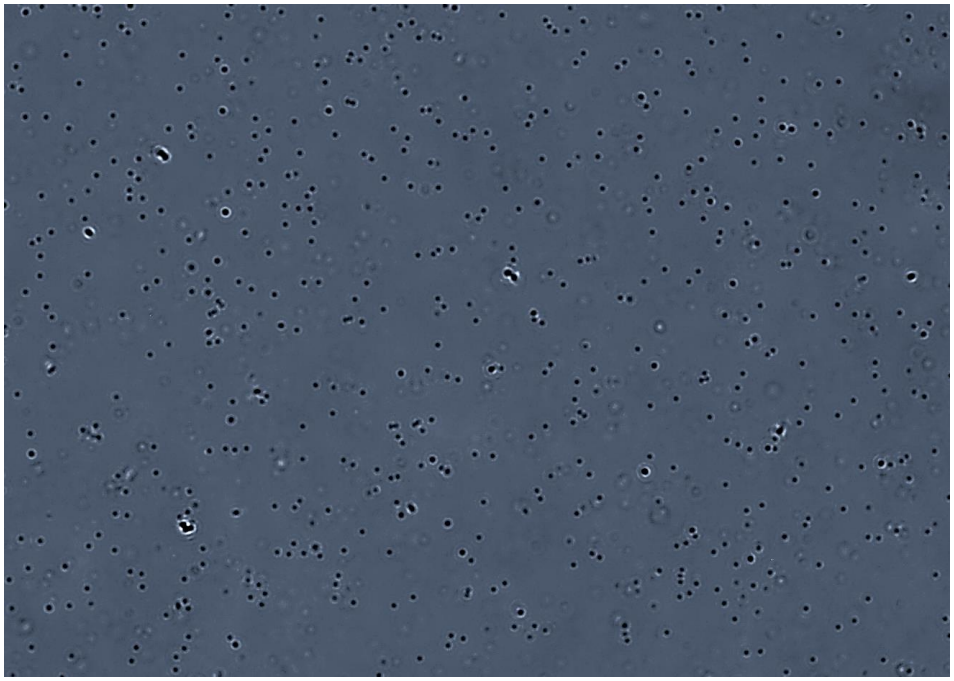

(a).

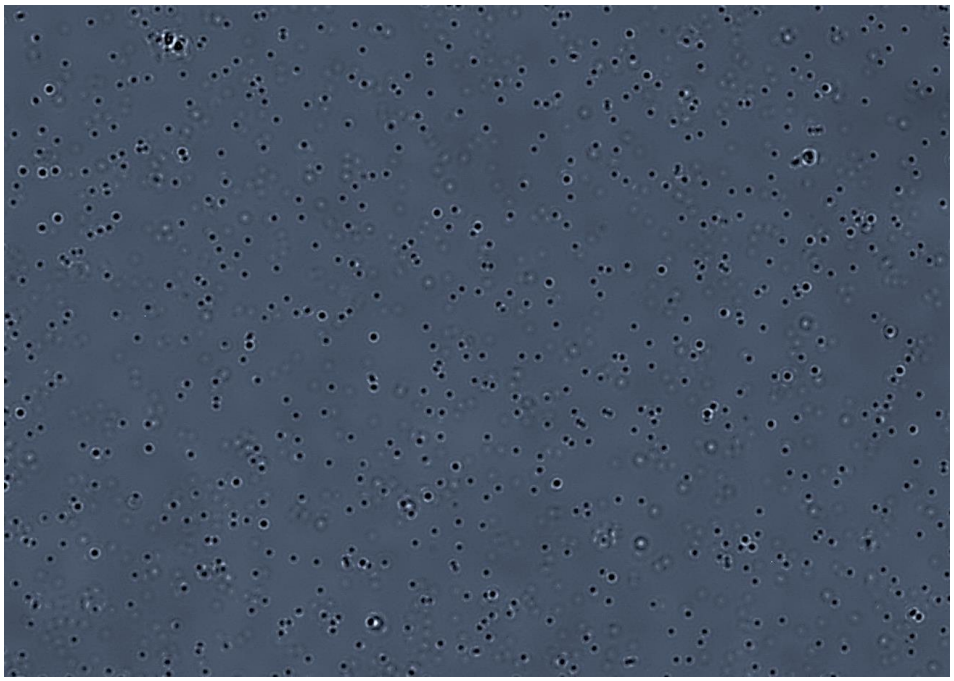

(b).

Figure 21. Images of PhyB and PIF3 mixed polystyrene beads at 40X magnification. (a). Mixture of PhyB and PIF3 on polystyrene beads (0.05 um diameter) irradiated at 740 nm to show disaggregation. (b). Mixture of PhyB and PIF3 on polystyrene beads irradiated at 660 nm to show aggregation.

Magnetic beads

It is difficult to determine if aggregation occurred when a mixture of PhyB magnetic beads and PIF3 magnetic beads were irradiated with red light. As seen in Figure 22, a few beads irradiated with red light seem to aggregate or form clumps, but this can also be seen under far-red light conditions and for plain magnetic beads as shown in Appendix D.

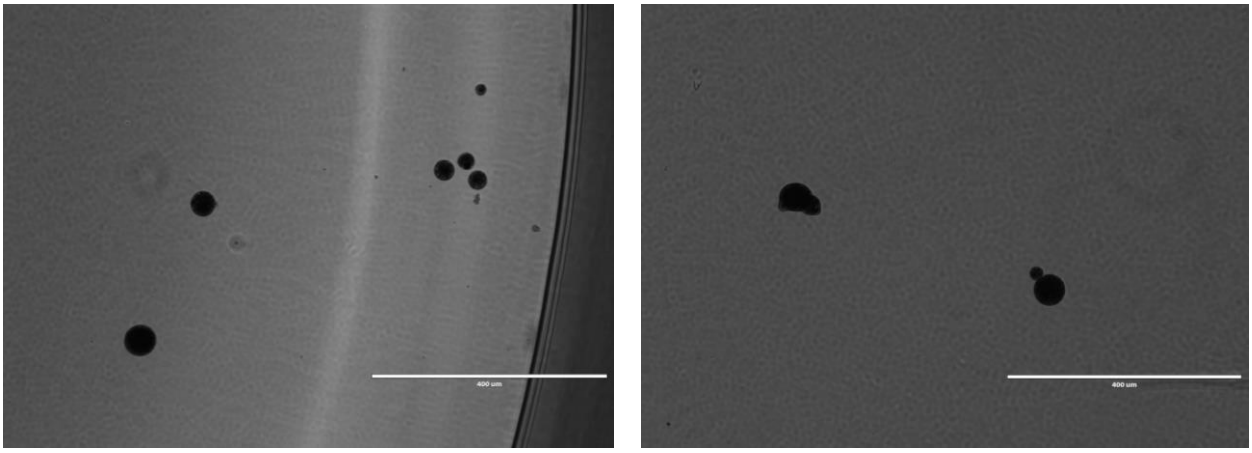

(a).

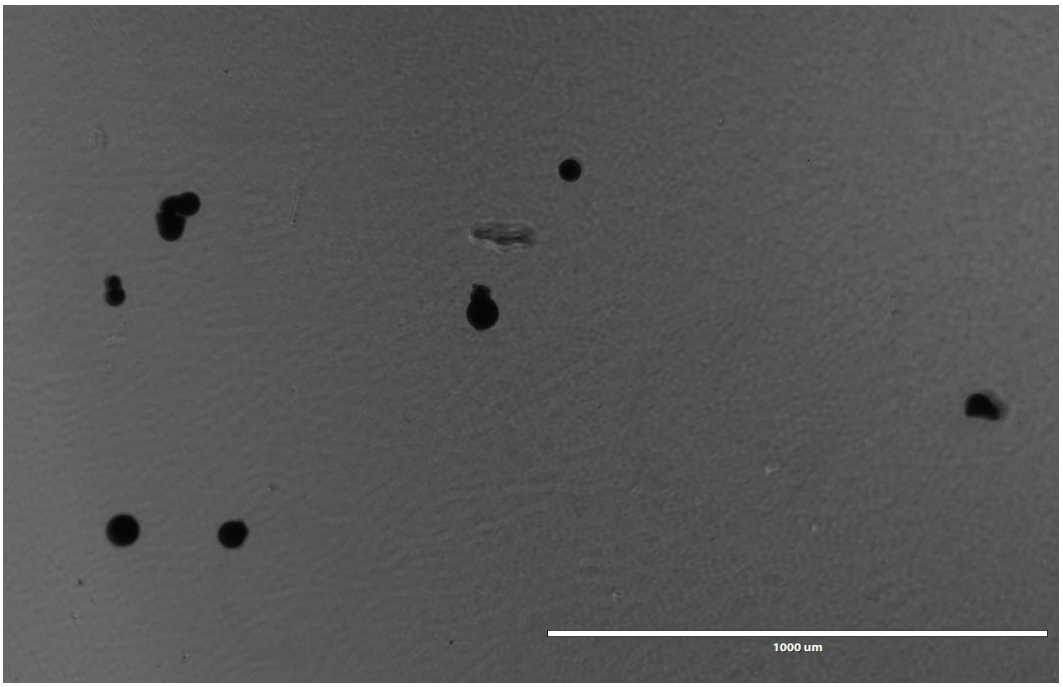

(b).

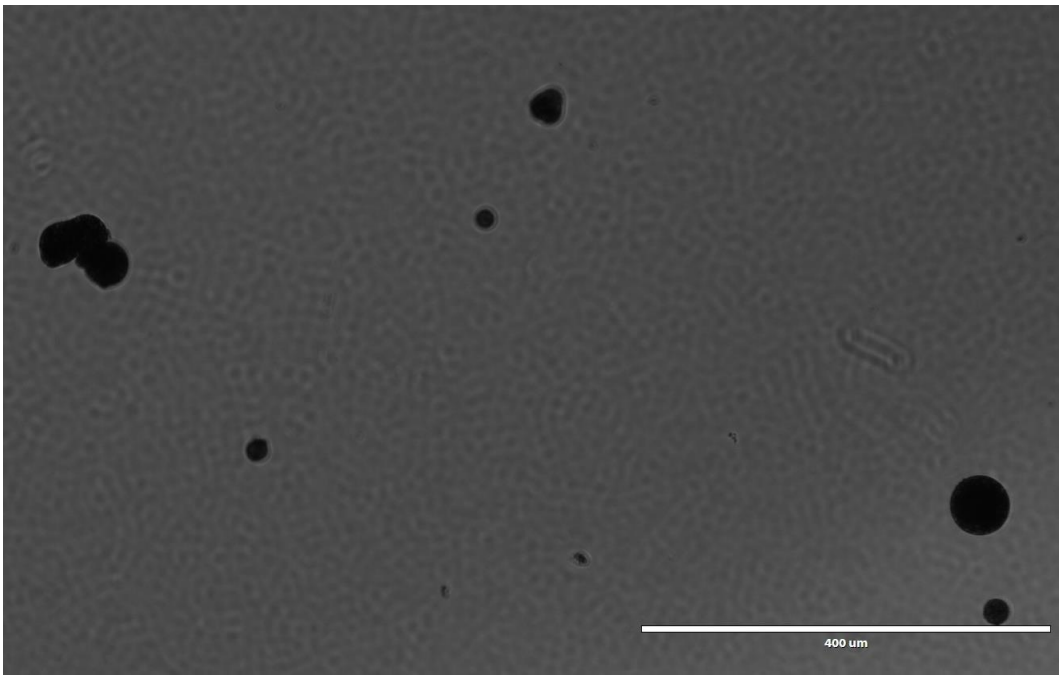

(c).

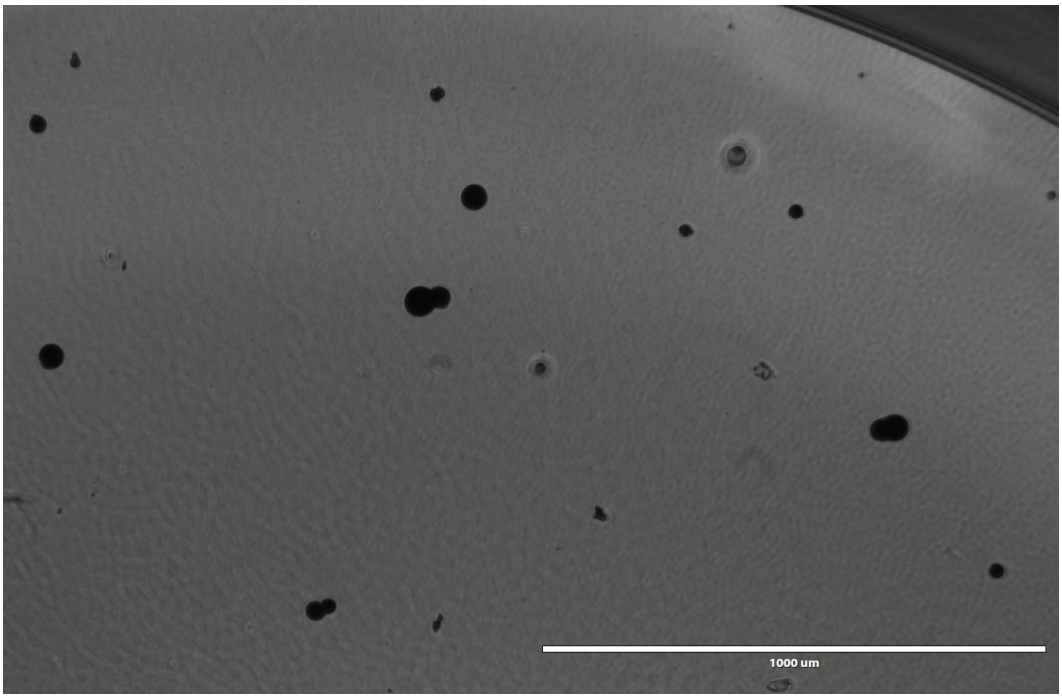

(d).

Figure 22. **PhyB and PIF3 mixed magnetic beads.** Images of a mixture of with PhyB on magnetic beads and PIF3 on magnetic beads. (a). Far-red light irradiation at 10X magnification. (b). Far-red light irradiation at 4X magnification. (c). Red light irradiation at 10X magnification. (d). Red light irradiation at 4X magnification.

CHAPTER 6: DISCUSSION

The development of nanotechnological devices and processes have increased in recent years and being able to control these at the nanoscale-level requires a high amount of specificity and characterization. Having a photo-switchable controlling protein complex would make it possible to create various devices for many biotechnology applications. Therefore, the overall goal of this research was to develop a platform using microparticles coated with PhyB and PIF3 proteins that would interact under the control of light by aggregating and disaggregating based on wavelength, intensity, and duration of light. For this project, characterizing the immobilization of PhyB and PIF3 on their respective surfaces was the basis for developing a photo-controllable platform. The histidine-tagged recombinant protein with a nickel-charged surface provided the specificity necessary for the platform design but expected results of bead aggregation and disaggregation influenced by red and far-red light sources of immobilized proteins were not observed in these experiments.

Expression of PhyB was achieved using the 5 L bioreactor. This provided control of the culture conditions for growing batch cultures of *E. coli* in unfavorable conditions of expressing three different proteins, of which two are toxic to the cells, using three different plasmids conferring resistance to three different antibiotics. The benchtop bioreactor provided control of temperature, pH, dissolved oxygen, and stir rate to provide favorable growth conditions for *E. coli* as well as overexpression conditions for the three proteins. However, production yield was low and the final purified protein concentration was 43.67 ug/mL for 10 grams of cell pellet per 830 mL of harvested cell media. A rather low yield of soluble recombinant protein using *E. coli* cells. These low yields of the truncated PhyB protein are due to the nature of the triple antibiotic culture containing two enzymes which are toxic to *E. coli* cells, but necessary to synthesize the

chromophore PΦB to react with the apo-PhyB to create a photo-responsive PhyB. According to the gels, the protein was estimated to be around 75% pure when eluted at the 250 mM imidazole fractions during IMAC purification.

Like the expression of PhyB, the expression of PIF3 was achieved using shake flask cultures, but the production yield was low and inconsistent with purified protein concentrated at 44.42 ug/mL for 8 grams of cell pellet per 2 L of harvested cell media. This may be due to the PIF3 ampicillin resistance-based plasmid construct. Beta-lactamase expression occurs in the plasmid to confer ampicillin resistance. The beta-lactamase is secreted into the cell media which inactivates the ampicillin. As the cells continue to proliferate under a decreasing concentration of ampicillin, the plasmid is no longer effective and results with inconsistent expression of protein in *E. coli.* Higher and consistent yields of PIF3 could be generated by using a kanamycin-based resistant plasmid construct.

The truncated version of PhyB used in these experiments displayed photo-responsive characteristics. The difference spectra displayed by this version of the PhyB produced the same results as reported in the literature to confirm the PhyB protein used in these experiments absorbed far-red and red light around 730 and 660 nm, respectively. This is a clear indication these experiments were conducted with photoactive PhyB, even with this truncated version. Furthermore, the light irradiance sensitivity data suggested more truncated PhyB absorbed light when irradiated at a higher intensity and for longer periods. Protein amounts of 0.1266 nmol of inactive and 0.1131 nmol of active PhyB absorbed light when considering the difference between the level 1 light intensity/30 second duration to level 5 light intensity/10 minute duration. However, the length of time the truncated PhyB was irradiated had more of an effect on PhyB absorption than the intensity of light. For instance, the difference between the level 5 light

intensity/10 minute duration and level 5 light intensity/30 second duration had 0.0485 nmol more inactive PhyB absorbed than the level 5 light intensity/10 minute duration and level 1 light intensity/10 minute duration. The same characteristic was seen with the active PhyB which suggests irradiation duration was a more contributing factor than the level of light intensity. These irradiation characteristics are significant for designing a photo-switchable protein complex if pulse duration were to be used as a controlling factor for aggregation and disaggregation. The dark reversion kinetics suggested the truncated PhyB reverted to its inactive form after red light irradiation in about 5 hours. It should be noted that 61.54% of 0.2426 nmol of PhyB reverted to its inactive form in the first hour. The kinetics results of these controlled conditions provide useful specifications as well as constraints when designing a photo-controllable platform. While 5 hours may seem like a rather long time, the bulk of the protein reverted into its inactive form within the first hour. This suggests the dependence of sustaining a critical concentration in the active form as part of a mechanism for different photoresponsive devices may require periodic pulses of red light to maintain desired active state levels.

The recombinant PhyB protein used for experiments was a truncated monomer version (72 kDa) of the natural full-length homodimer protein (129 kDa). This truncated protein was shown to be photosensitive as well as photoreactive with PIF3, albeit a weaker interaction than the full-length homodimer (4). The rationale for using the truncated PhyB version was to achieve a higher yield of soluble and active protein than what may be achieved using the full-length homodimer version. A second rationale was the truncated version of the protein would have a smaller immobilized footprint on the surface of the beads that would allow for a higher surface packing density leading to a higher level of photoactive control.

The photoresponsiveness and photoactivity of this truncated holo-PhyB protein was achieved by the autocatalytic covalent attachment of PΦB to apo-PhyB when expressed in *E. coli*. The photo-responsive characteristics were present in the truncated PhyB based on difference spectra measurements and specific immobilization to polystyrene and magnetic beads was also achieved via the genetically appended histidine-tag on the proteins and the nitrilotriacetic acid chelated Ni^{2+} on the microparticles. However, the depletion assay for PhyB polystyrene beads suggests the truncated PhyB was immobilized to polystyrene beads, but this truncated monomer structure was possibly unable to extend the PIF3 binding site into solution and make it available to allow binding of PIF3. Even with PIF3 immobilized on polystyrene beads, binding of PhyB in solution to the immobilized PIF3 was undetectable suggesting two possibilities: first the F108-NTA Pluronic surfactant may have degraded due to its shelf life and wasn't specifically immobilizing the protein on the surface, but rather allowing it to denature on the surface, rendering it biologically inactive; and second the truncated PhyB binding site on the immobilized PIF3 protein was blocked and not extended into the solution away from the surface. These results prompted a change in the immobilization scheme in an attempt to remove the unknown issue: if the proteins are specifically binding to the surface and remaining photo-responsive.

With the inconsistent results using the polystyrene beads, NTA agarose-coated magnetic particles proteins were used to specifically immobilize the proteins. These magnetic agarose beads are designed to be used for quick purification of histidine-tagged recombinant proteins without having to use a more time-consuming gravity fed column. The rationale for using these particles is they allow specific protein immobilization on the surface while limiting non-specific interaction via the hydrophilic agarose coating. To reiterate, these particles were designed to

limit non-specific binding during purification procedures and only allow histidine-tag binding for quick, high purity runs. These are the exact needs for this photocontrollable platform.

The depletion assays using the magnetic agarose beads displayed consistent increases of PhyB immobilized on the surface based on less protein remaining in the supernatant. Activity of the immobilized PhyB after irradiation with red light suggested immobilized protein may be accounted for during the depletion assay using magnetic beads and binding was possible to immobilized protein. PIF3 also had around 25% more protein immobilized to the magnetic beads than the polystyrene beads signifying the ineffectiveness of the aged F108 Pluronic surfactant. This may have assisted with the binding of PhyB in solution as more protein was depleted with PIF3 immobilized to the surface rather than PhyB immobilized to the surface indicating the binding site for the truncated PhyB may not be as readily available once irradiated with red light. When the volume of PIF3 increased for further magnetic bead depletion assays as shown in Appendix C, more PhyB in solution was depleted from immobilized PIF3 once irradiated with red light. This trend was not mimicked in the opposite configuration of immobilized PhyB on magnetic beads with increased volume of PIF3 which would again indicate the active form of the truncated PhyB is inhibited when immobilized. The various sizes of magnetic beads in the provided stock could present some challenges in fine tuning protein concentration surface coverage, but imaging the magnetic beads was more efficient than using the polystyrene beads.

The technique used to image the polystyrene and magnetic beads presented the challenge of confirming aggregation occurred when using both sets of protein. Images of a mixture with truncated PhyB on beads and PIF3 on beads were similar to images of plain beads which made it difficult to conclude disaggregation and aggregation occurred when irradiated with far-red and

red light, respectively. The size of the polystyrene beads made it difficult to capture any disaggregation and aggregation, but the ineffectiveness of the F108 Pluroinc surfactant was also a contributing factor. The magnetic beads were much easier to image due to their size, but capturing aggregation between magnetic particles was inconclusive because 'clumped' beads may have be resting on one another and not through PhyB and PIF3 binding. Incorporating a fluorescent marker to each protein would assist in imaging disaggregation and aggregation in real time if immobilization to the beads and protein conformational changes are unaffected by the marker. Therefore, future experiments would incorporate the fluorescent marker during bead imaging along with using a photo-responsive full-length holo-PhyB and kanamycin based PIF3 plasmid during expression and bead characterization experiments to achieve a photo-switchable controlling mechanism.

CHAPTER 7: FUTURE RESEARCH

The future research will consider the same specific aims featured in this work, but using full-length PhyB and PIF3, rather than the truncated versions used in this study, to achieve a higher binding affinity between the two full-length proteins. Protein immobilization will also be done using the magnetic beads. However, the binding saturation threshold needs to be first established to ensure all binding sites on the beads are bound with the intended immobilized protein. This immobilization saturation will inhibit the counter protein in solution to interact with NTA-Ni^{2+} binding sites, as they would be unavailable, and instead interact photoreversibly with the immobilized protein. The procedures for Specific Aims 1 and 5 will incorporate additional work while Specific Aims 2, 3, and 4 will remain the same, but contain full-length PhyB and PIF3. Specific Aims 1 and 5 are listed below:

Specific Aim 1. Convert full-length PhyB and PIF3 to kanamycin-resistant plasmids. Perform triple-transformation of plasmids for full-length apo-PhyB, heme oxygenase, and PΦB synthase in *E. coli* BL21(DE3) cells. Design growth conditions in bioreactor and overexpress and purify recombinant full-length PhyB and PIF3. A full-length apo-PhyB and PIF3 are available in the East Carolina University Bioprocess Engineering Laboratory, but both are in ampicillin-resistant plasmids. Both proteins must first be converted to kanamycin-resistant plasmids to establish more stable production yields. The full-length apo-PhyB will then be transformed in DH5α *E. coli* cells to ensure plasmid propagation and stability. The heme oxygenase and phytochrombilin PΦB synthase have already been transformed in DH5α *E. coli* cells. Similarly, the full-length PIF3 kanamycin-resistant plasmid will be transformed in DH5α *E. coli.* A triple-transformed cell stock consisting of the histidine-tagged full-length apo-PhyB, heme oxygenase (HO1), and phytochromobilin PΦB synthase will be coexpressed in BL21(DE3) *E. coli* to make

a full-length holo-PhyB product. Production and purification of full-length holo-PhyB and PIF3 will be done as stated in previous specific aims for this research.

Specific Aim 5. Characterize photo-induced aggregation and disaggregation of polystyrene nanoparticle suspensions.

The future goal for this project is to develop and characterize a colloidal suspension of full-length PhyB and PIF3 which when irradiated with red and far-red light will aggregate and disaggregate respectively. To achieve this goal, the transient state dynamics and steady state conditions for light-induced aggregation, light-induced disaggregation, dark reversion-based disaggregation, and pulse with modulation of concurrent red and far-red light to maintain intermediate levels of aggregation will need to be characterized. Proteins will be tagged with their own fluorescent marker to image protein immobilization to magnetic beads as another way of characterizing the immobilization on the beads. Each procedure is detailed below:
Characterize red light-induced aggregation dynamics: The aggregation dynamics of the colloidal suspension will be analyzed by two approaches: imaging it at low concentrations and measuring optical density at high concentrations. To image the colloidal suspension at low nanoparticle concentrations, the use of glass depression slides and an inverted microscope will be used. Two images for each sample will be taken at different wavelengths. These wavelengths are based off the maximum and minimum absorption spectra of the PhyB and not the red and far-red wavelengths for conformational switching. To remove background noise and achieve optimal image contrast, differential images will be taken from the two images. These two images will allow for the quantification of aggregated colloidal suspensions as a function of time and red light irradiance. Measuring the optical density (turbidity in this case) using a

spectrophotometer of the colloidal suspensions at high concentrations will provide a quantifiable aggregation as a function of time and red light irradiance.

Experimental conditions such as pH, temperature, viscosity, nanoparticle concentration, etc. will be investigated to characterize the dynamics of PhyB/PIF3 aggregation. The suspensions of PhyB/PIF3 nanoparticles will be saturated with far-red light to induce an inactive conformation of PhyB to achieve steady state and then irradiated with red light to initiate aggregation.

Characterize far-red light-induced disaggregation dynamics: The disaggregation dynamics of the colloidal suspension will be analyzed with the same experimental approach as in the aggregation dynamics. Differential images and spectrophotometric measurements will be used to quantify disaggregation based off time and far-red light irradiance. Experimental conditions such as pH, temperature, viscosity, nanoparticle concentration, etc. will be investigated to characterize the dynamics of PhyB/PIF3 disaggregation. The suspensions of PhyB/PIF3 nanoparticles will be saturated with red light to induce an active conformation of PhyB to achieve steady state and then irradiated with far-red light to initiate disaggregation.

Characterize dark reversion-based disaggregation dynamics: Dark reversion-based disaggregation will be characterized by analyzing the influences of the conformational change of PhyB from Pfr to Pr during transient and steady states. This experiment can be done during the end of characterizing the aggregation dynamics. Images of the colloidal suspensions will be taken during the steady state of aggregation and an absorbance measurement will be taken to quantify the dark reversion disaggregation kinetics.

Characterize irradiation pulse width for controlling aggregation: Red and far-red light will be pulsed intermittently to the colloidal suspensions to test the intermediate levels of aggregation. This will help maintain steady state conditions of the colloidal suspensions. Any patterns of pulse trains delivered to the suspensions, such as duty cycles and synchronization can be used to correlate with a given intermediate aggregation level. Therefore, tunable conditions could be established to transition between intermediate levels by adjusting the duty cycles of light pulses. Images and absorbance measurements will also be taken during these intermittent pulse waves to quantify and monitor the transient and steady states.

Image aggregate structures: Morphological images of the aggregated colloidal suspension will be taken using the same approach as in characterizing the aggregation dynamics. Examining the static and dynamic structures of these colloidal suspensions could be used as building blocks to create functional materials at the macroscopic level through programmable delivery of light signals. Mixtures of different sized nanoparticles at different concentration ratios can be used to create unique structures.

Future Research Conclusion

As stated before, the overall goal for this work is to create a photocontrollable platform to regulate the disaggregation and aggregation of microparticle suspensions upon irradiation with far-red and red light respectively with PhyB and PIF3 as the backbone for the switching mechanism. The truncated PhyB presented problems with binding to PIF3 when it was immobilized to a surface which made it difficult to detect aggregation and disaggregation. Therefore, using a full-length PhyB and kanamycin-resistant PIF3 could lead to more consistent

results when considering binding affinity between the two proteins and the larger footprint of PhyB on the bead surface to hopefully develop photocontrollable devices.

REFERENCES

1. Quail PH. Phytochromes. *Current Biology*. 2010;20(12):R507.

2. Medzihradszky M, Bindics J, Ádám É, et al. Phosphorylation of phytochrome B inhibits light-induced signaling via accelerated dark reversion in arabidopsis. *The Plant Cell*. 2013;25(2):535-544.

3. Burgie ES, Bussell AN, Walker JM, Dubiel K, Vierstra RD. Crystal structure of the photosensing module from a red/far-red light-absorbing plant phytochrome. Proc Natl Acad Sci U S A. 2014 Jul 15;111(28):10179-84.

4. Ni M, Tepperman JM, Quail PH. Binding of phytochrome B to its nuclear signalling partner PIF3 is reversibly induced by light. *Nature*. 1999;400(6746):781-784.

5. Quail PH. Phytochrome-interacting factors. *Seminars in Cell and Developmental Biology*. 2000;11(6):457-466.

6. Martínez-García JF, Huq E, Quail PH. Direct targeting of light signals to a promoter element-bound transcription factor. *Science*. 2000;288(5467):859-863.

7. Ni M, Tepperman JM, Quail PH. PIF3, a phytochrome-interacting factor necessary for normal photoinduced signal transduction, is a novel basic helix-loop-helix protein. *Cell*. 1998;95(5):657-667.

8. Bienert S, Waterhouse A, de Beer TA, Tauriello G, Studer G, Bordoli L, Schwede T. The SWISS-MODEL Repository-new features and functionality. Nucleic Acids Res. 2017 Jan 4;45(D1):D313-D319.

9. Li J, Li G, Wang H, Wang Deng X. Phytochrome signaling mechanisms. *The arabidopsis book*. 2011;9:e0148.

10. Zhu Y, Tepperman JM, Fairchild CD, Quail PH. Phytochrome B binds with greater apparent affinity than phytochrome A to the basic helix-loop-helix factor PIF3 in a reaction requiring the PAS domain of PIF3. *Proceedings of the National Academy of Sciences of the United States of America*. 2000;97(24):13419-13424.

11. Zhang J, Stankey RJ, Vierstra RD. Structure-guided engineering of plant phytochrome B with altered photochemistry and light signaling. *Plant Physiology*. 2013;161(3):1445-1457.

12. Rockwell NC, Su Y, Lagarias JC. Phytochrome structure and signaling mechanisms. *Annual Review of Plant Biology*. 2006;57(1):837-858

13. Mukougawa K, Kanamoto H, Kobayashi T, Yokota A, Kohchi T. Metabolic engineering to produce phytochromes with phytochromobilin, phycocyanobilin, or phycoerythrobilin chromophore in escherichia coli. *FEBS Letters*. 2006;580(5):1333-1338.

14. Wahleithner JA, Li L, Lagarias JC. Expression and assembly of spectrally active recombinant holophytochrome. *Proceedings of the National Academy of Sciences of the United States of America*. 1991;88(23):10387-10391.

15. Quail PH, Huq E, Shimizu-Sato S, Tepperman JM. A light-switchable gene promoter system. *Nature Biotechnology*. 2002;20(10):1041-1044.

16. Leung DW, Otomo C, Chory J, Rosen MK. Genetically encoded photoswitching of actin assembly through the Cdc42-WASP-Arp2/3 complex pathway. *Proceedings of the National Academy of Sciences of the United States of America*. 2008;105(35):12797-12802.

17. Ni W, Xu S, González-grandío E, et al. PPKs mediate direct signal transfer from phytochrome photoreceptors to transcription factor PIF3. *Nature Communications*. 2017; 8:15236.

18. Bodratti AM, Alexandridis P. Formulation of poloxamers for drug delivery. *Journal of functional biomaterials*. 2018;9(1):11.

19. Pitto-Barry A, Barry N, Pluronic block-copolymers in medicine: from chemical and biological versatility to rationalization and clinical advances. *Polymer* Chemistry., 2014, 5, 3291-3297. ISSN 1759-9954.

20. Ho C, Limberis L, Caldwell KD, Stewart RJ. A metal-chelating pluronic for immobilization of histidine-tagged proteins at interfaces: Immobilization of firefly luciferase on polystyrene beads. *Langmuir*. 1998;14(14):3889-3894.

21. Lam AT, Tsitkov S, Zhang Y, Hess H. Reversibly bound kinesin-1 motor proteins propelling microtubules demonstrate dynamic recruitment of active building blocks. *Nano letters*. 2018;18(2):1530-1534.

APPENDIX A: PROTEIN CONCENTRATION

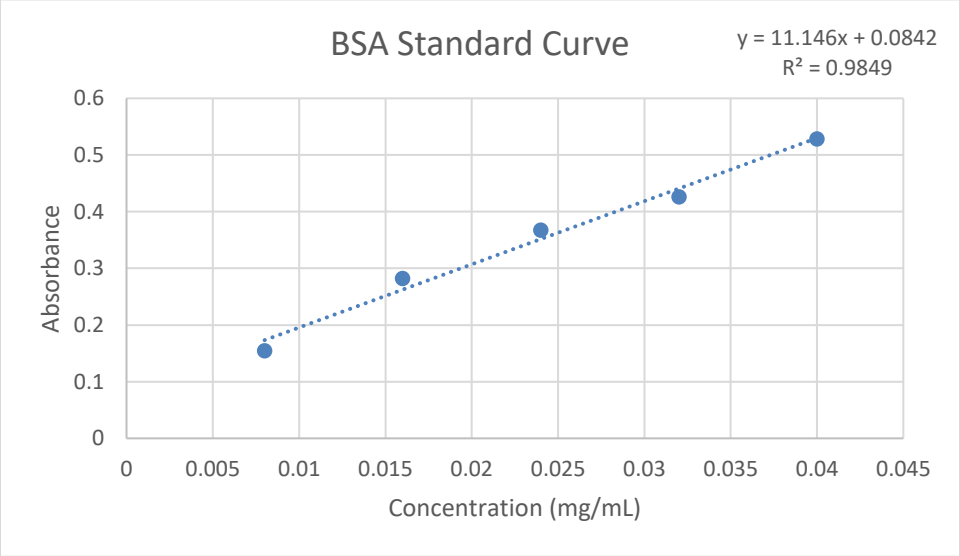

Figure 23. BSA standard curve. Absorbance was measured for each BSA concentration of 0.04, 0.032, 0.024, 0.016, and 0.08 mg/mL.

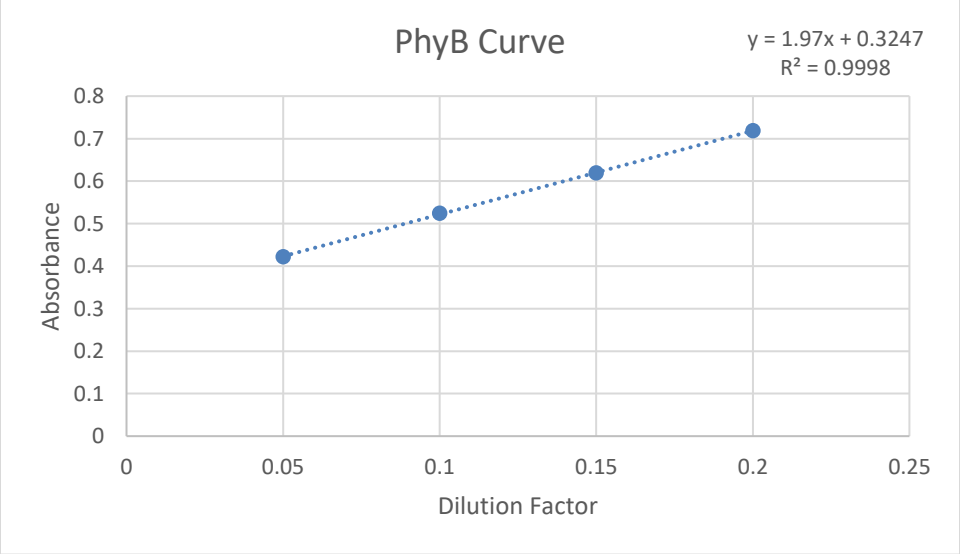

Figure 24. PhyB curve. Absorbance was measure for each dilution factor of PhyB at 0.2, 0.15, 0.1, and 0.05 to compare with the BSA standard curve. Concentration of PhyB was calculated at 43.67 ug/mL.

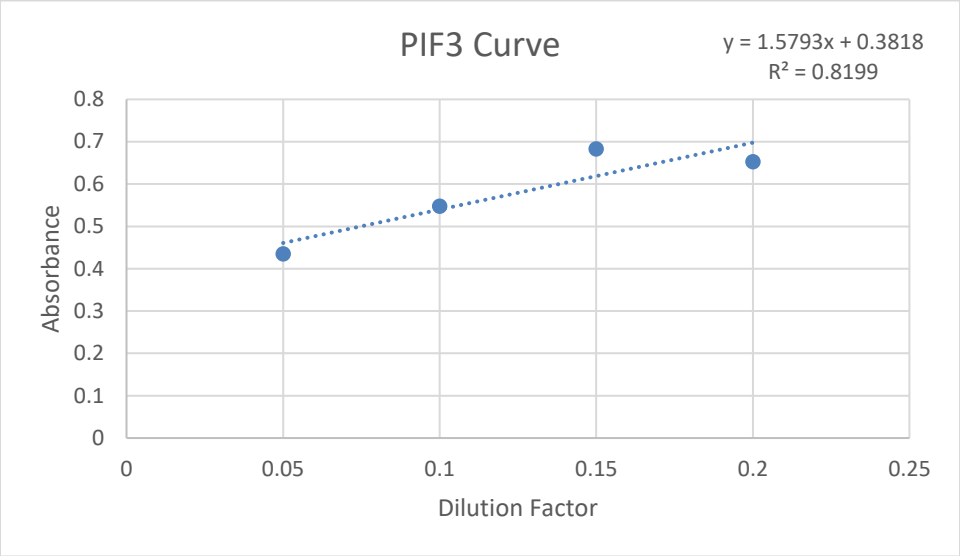

Figure 25. PIF3 curve. Absorbance was measure for each dilution factor of PIF3 at 0.2, 0.15, 0.1, and 0.05 to compare with the BSA standard curve. Concentration of PhyB was calculated at 44.42 ug/mL.

APPENDIX B: COOMASSIE STAINING AND DESTAINING

Reagents needed:

Coomassie Stain solution

Destain solution

Kimwipes (or something else to absorb the coomassie)

a microwave (optional)

Directions:

1. Remove SDS-PAGE gel from glass and rinse once in ddH_2O in a suitable container with a lid. Try not to use a container much larger or much smaller than the gel.
2. Add enough Coomassie Stain to cover the gel by 1/2 inch (~ 1.5 cm).
3. Microwave on high power for 40 seconds to 1 minute (until the Coomassie Stain boils).
4. Incubate the gel in the Coomassie stain for 5 to 10 minutes on a rocking table. If you did not microwave the Coomassie/gel, incubate for at least 1 hour.
5. Pour off the Coomassie Stain. The Coomassie Stain can be recycled a couple of times by filtering it.
6. Rinse twice in ddH_2O or used Destain solution to remove Coomassie Stain from the container.
7. Add fresh Destain solution to cover the gel by 3/4 inch (~ 2 cm).
8. Tie Kimwipes in a simple knot and place 4 of them in the Destain solution around the gel. Try to avoid laying the Kimwipes on the gel as this will cause an uneven destaining.
9. Microwave on high power for 40 seconds to 1 minute (until the Destain boils).
10. Incubate the gel in the Destain solution for 10 minutes on a rocking table. If you did not microwave the Coomassie/gel, incubate for at least 1 hour.
11. Discard the stained Kimwipes and replace with fresh knotted Kimwipes.
12. Incubate a second time for 10 minutes to overnight on a rocking table. Stop whenever the level of destaining is sufficient for you. Microwave again to speed up the process.
13. The used Destain solution can be recycled a couple of times by storing it in a sealed container with sponges or Kimwipes to remove all traces of Coomassie Stain.

<u>Coomassie Stain - 1 L</u>

0.1% Coomassie R250, 10% acetic acid, 40% methanol

Reagents needed:

1g	Coomassie R250
100 mL	glacial acetic acid
400 mL	methanol

500 mL ddH_2O

Directions:

1. Add 100 mL of glacial acetic acid to 500 mL of ddH_2O.
2. Add 400 mL of methanol and mix.
3. Add 1g of Coomassie R250 dye and mix.
4. Filter to remove particulates (a coffee filter works great for this and is cheap)
5. Store at room temperature in a sealable container.

De-Stain for Coomassie - 1 L

20% methanol, 10% acetic acid

Reagents needed:

200 mL methanol

100 mL glacial acetic acid

700 mL ddH_2O

Directions:

1. Add 100 mL of glacial acetic acid to 700 mL of ddH_2O.
2. Add 200 mL of methanol and mix.
3. Store at room temperature in a sealable container.

APPENDIX C: DEPLETION ASSAY OF PLAIN BEADS

Polystyrene Bead Depletion Assay

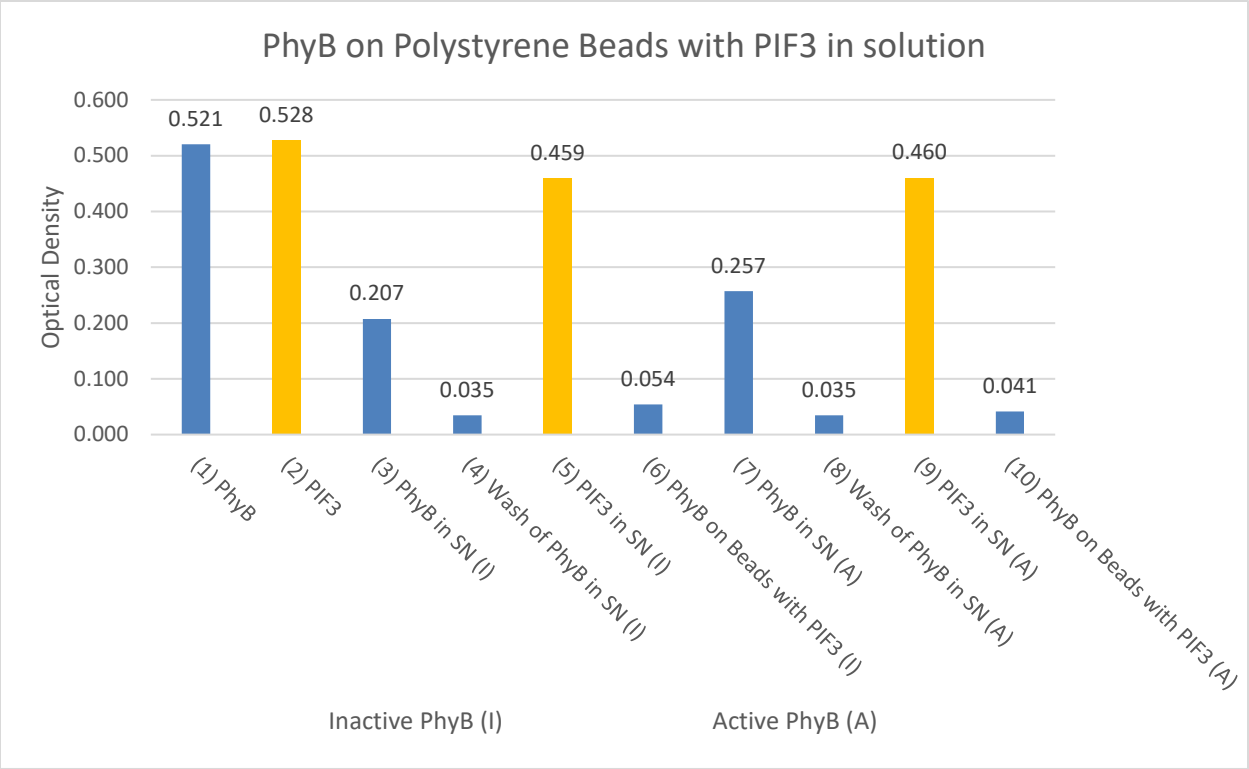

(a).

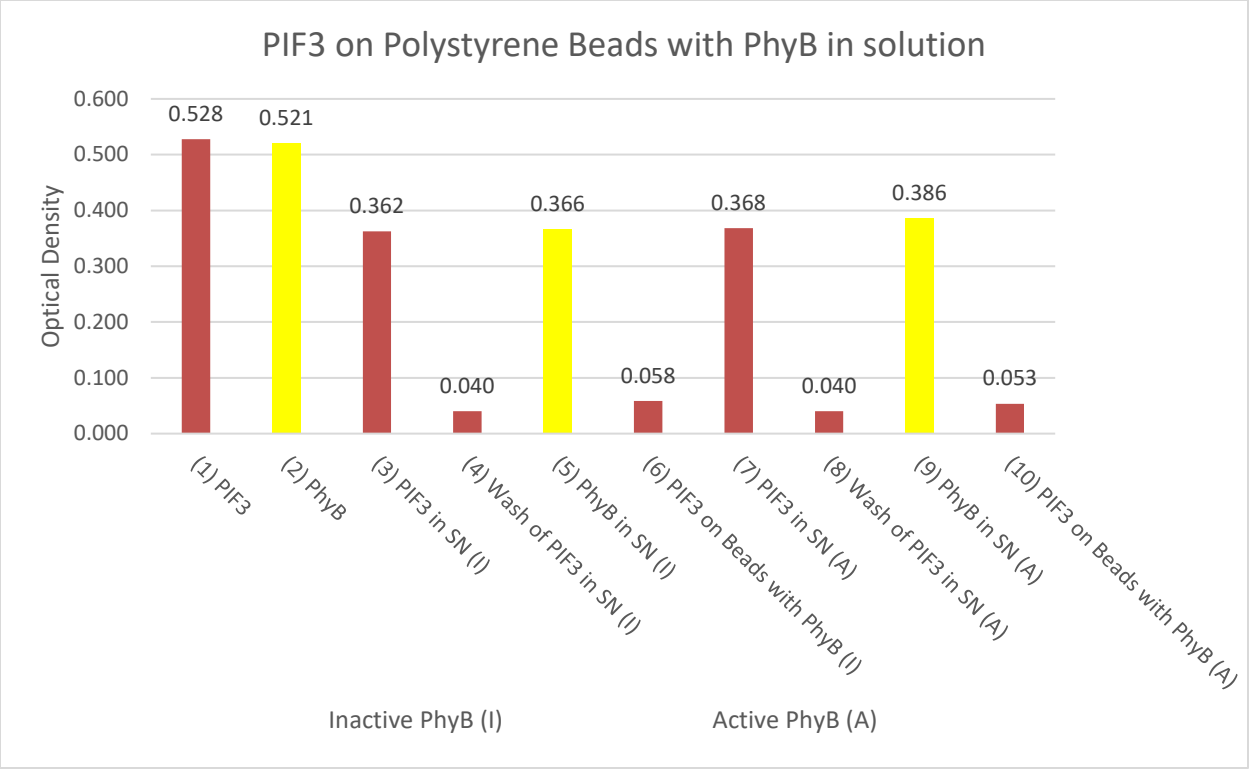

(b).

Figure 26. Depletion assay for 1:1 ratio of PhyB:PIF3 with Polystyrene Beads. (a). 50 uL of 43.67 ug/mL PhyB immobilized on 0.01% polystyrene beads with 50 uL of 44.42 ug/mL PIF3 in solution. (b). 50 uL of 44.42 ug/mL PIF3 immobilized on 0.01% polystyrene beads with 50 uL of 43.67 ug/mL PhyB in solution. Inactive (I) and active (A) PhyB represent the samples contained the Pr and Pfr form of PhyB, respectively. Lane 1 – 50 uL of protein added to polystyrene beads. Lane 2 – 50 uL of protein in solution. Lane 3 and 7 – Amount of protein referenced to lane 1 not immobilized. Lane 4 and 8 – Residual protein after polystyrene bead wash. Lane 5 and 9 – Amount of protein in solution referenced to lane 2 after irradiation of far-red and red light respectively. Lane 6 and 10 – Amount of protein immobilized on polystyrene beads after irradiation of far-red and red light respectively.

Magnetic Bead Depletion Assay

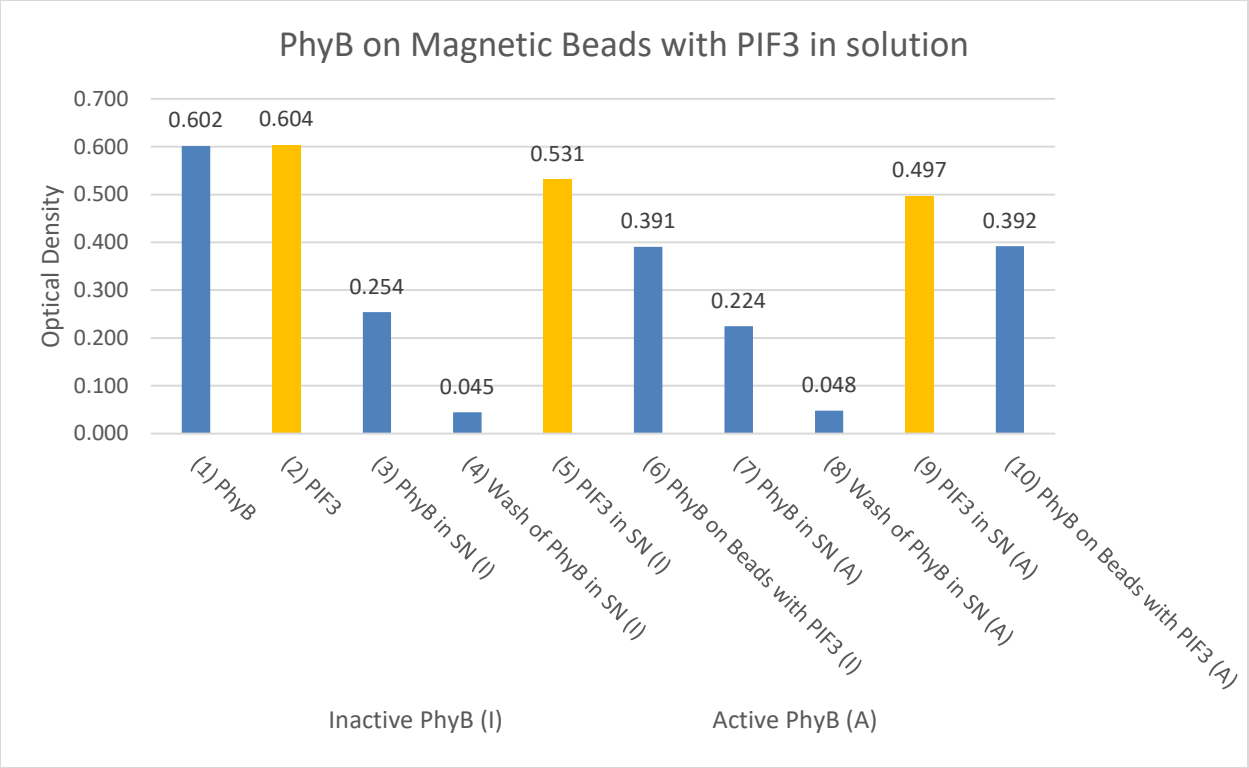

(a).

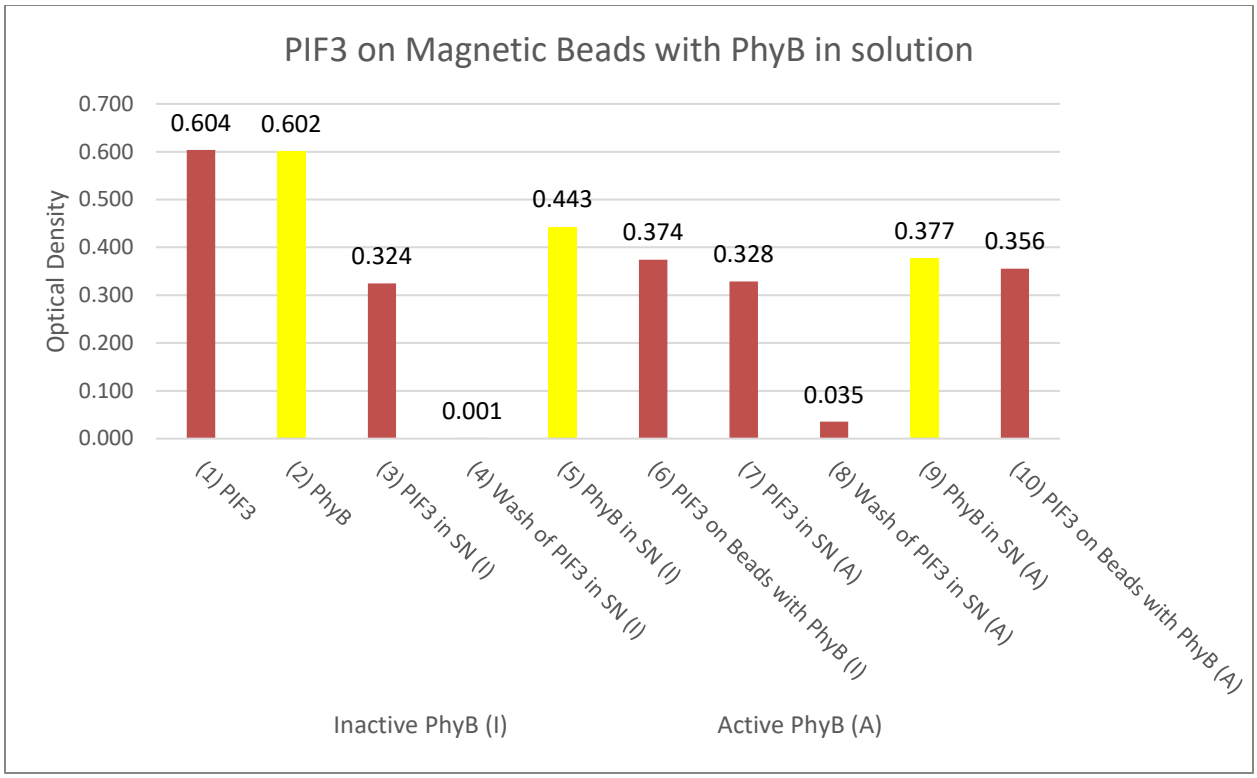

(b).

Figure 27. Depletion assay for 1:1.5 ratio of PhyB:PIF3 with Magnetic Beads. (a). 50 uL of 43.67 ug/mL PhyB immobilized on 10 uL of 5% magnetic beads with 75 uL of 44.42 ug/mL PIF3 in solution. (b). 75 uL of 44.42 ug/mL PIF3 immobilized on 10 uL of 5% magnetic beads with PhyB in solution. Inactive (I) and active (A) PhyB represent the samples contained the Pr and Pfr form of PhyB, respectively. Lane 1 – Protein added to magnetic beads. Lane 2 – Protein in solution. Lane 3 and 7 – Amount of protein referenced to lane 1 not immobilized. Lane 4 and 8 – Residual protein after magnetic bead wash. Lane 5 and 9 – Amount of protein in solution referenced to lane 2 after irradiation of far-red and red light respectively. Lane 6 and 10 – Amount of protein immobilized on magnetic beads after irradiation of far-red and red light respectively.

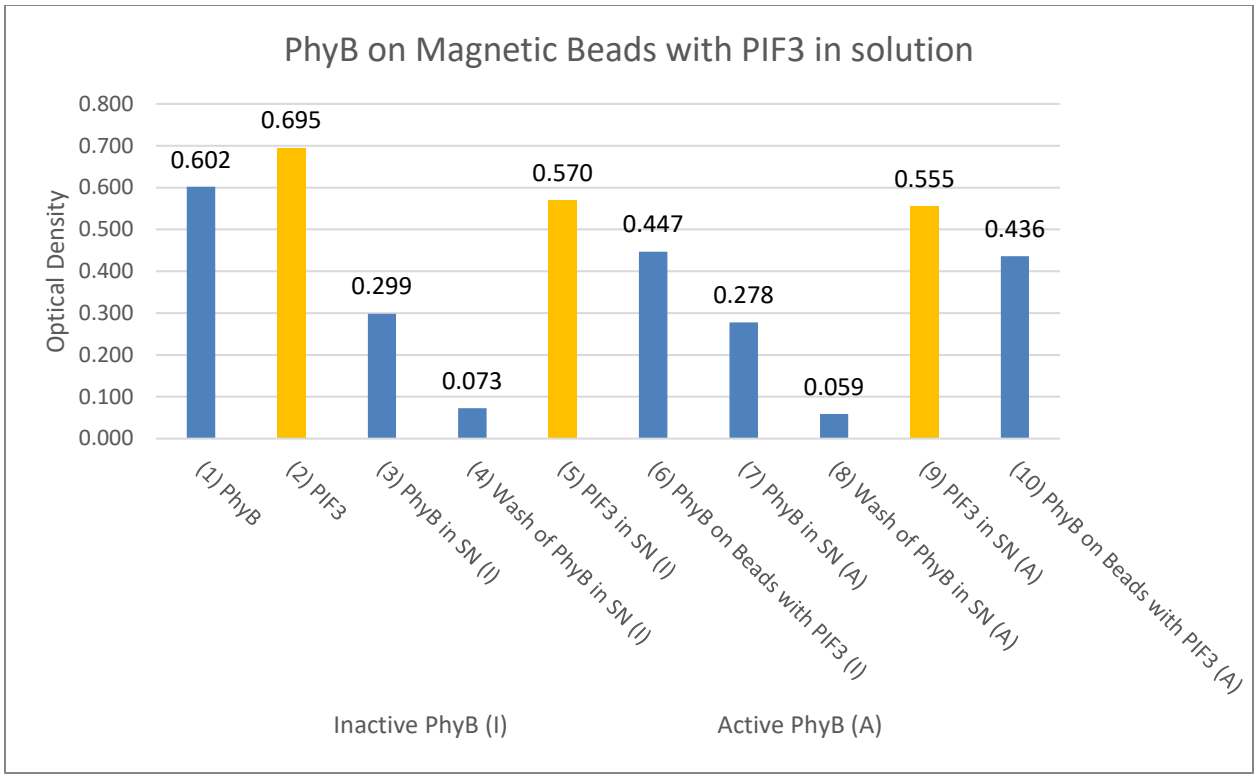
PhyB on Magnetic Beads with PIF3 in solution
Optical Density
0.800
0.700
0.600
0.500
0.400
0.300
0.200
0.100
0.000
0.602
0.695
0.299
0.073
0.570
0.447
0.278
0.059
0.555
0.436
(1) PhyB
(2) PIF3
(3) PhyB in SN (I)
(4) Wash of PhyB in SN (I)
(5) PIF3 in SN (I)
(6) PhyB on Beads with PIF3 (I)
(7) PhyB in SN (A)
(8) Wash of PhyB in SN (A)
(9) PIF3 in SN (A)
(10) PhyB on Beads with PIF3 (A)
Inactive PhyB (I)
Active PhyB (A)

(a).

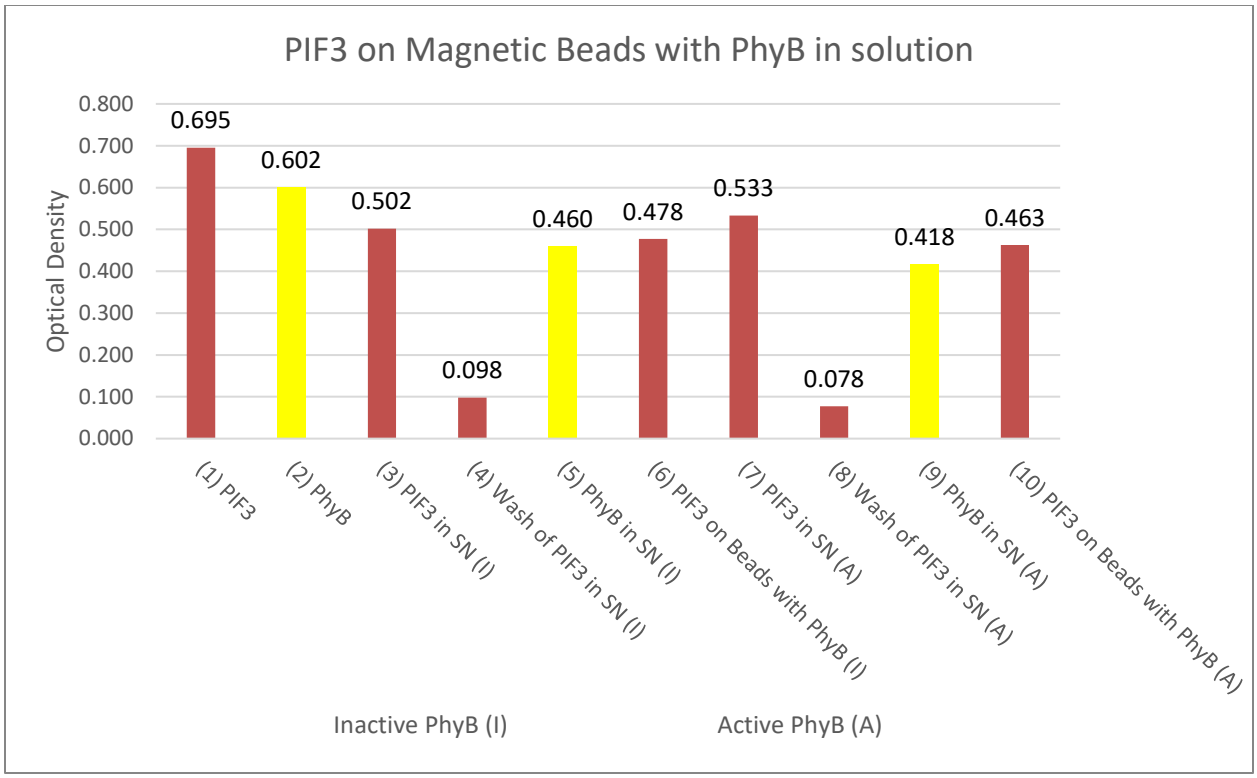

(b).

Figure 28. Depletion assay for 1:2 ratio of PhyB:PIF3 with Magnetic Beads. (a). 50 uL of 43.67 ug/mL PhyB immobilized on 10 uL of 5% magnetic beads with 100 uL of 44.42 ug/mL PIF3 in solution. (b). 100 uL of 44.42 ug/mL PIF3 immobilized on 10 uL of 5% magnetic beads with PhyB in solution. Inactive (I) and active (A) PhyB represent the samples contained the Pr and Pfr form of PhyB, respectively. Lane 1 – Protein added to magnetic beads. Lane 2 – Protein in solution. Lane 3 and 7 – Amount of protein referenced to lane 1 not immobilized. Lane 4 and 8 – Residual protein after magnetic bead wash. Lane 5 and 9 – Amount of protein in solution referenced to lane 2 after irradiation of far-red and red light respectively. Lane 6 and 10 – Amount of protein immobilized on magnetic beads after irradiation of far-red and red light respectively.

APPENDIX D: IMAGES OF PLAIN BEADS

Polystyrene Bead Images

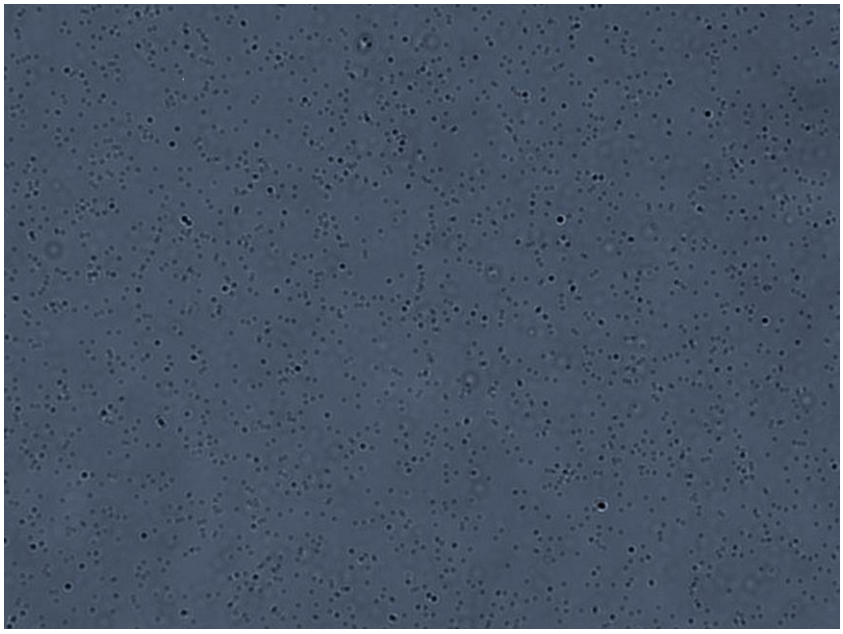

(a).

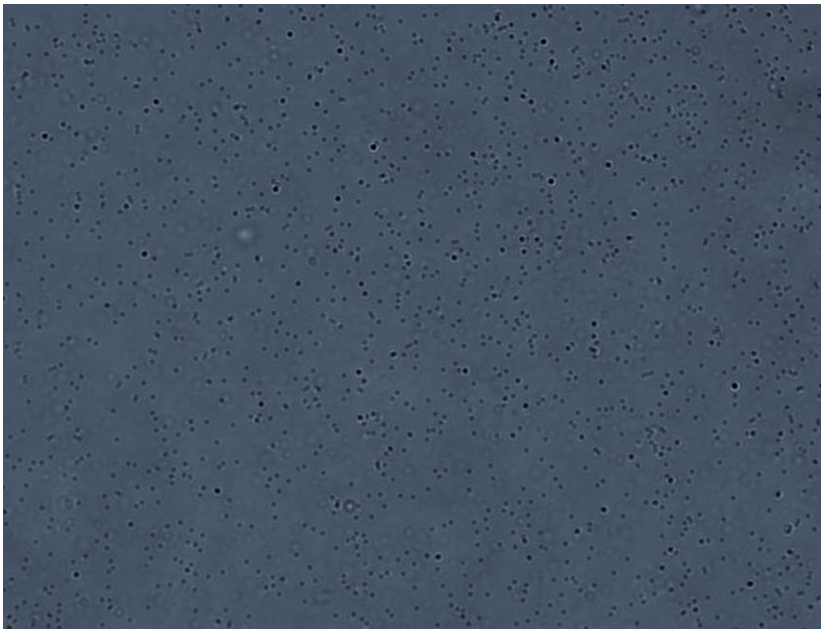

(b)

Figure 29. Images of polystyrene beads at 40X magnification. (a). Polystyrene beads irradiated at 740 nm. (b). Polystyrene beads irradiated at 660 nm.

Magnetic Bead Images

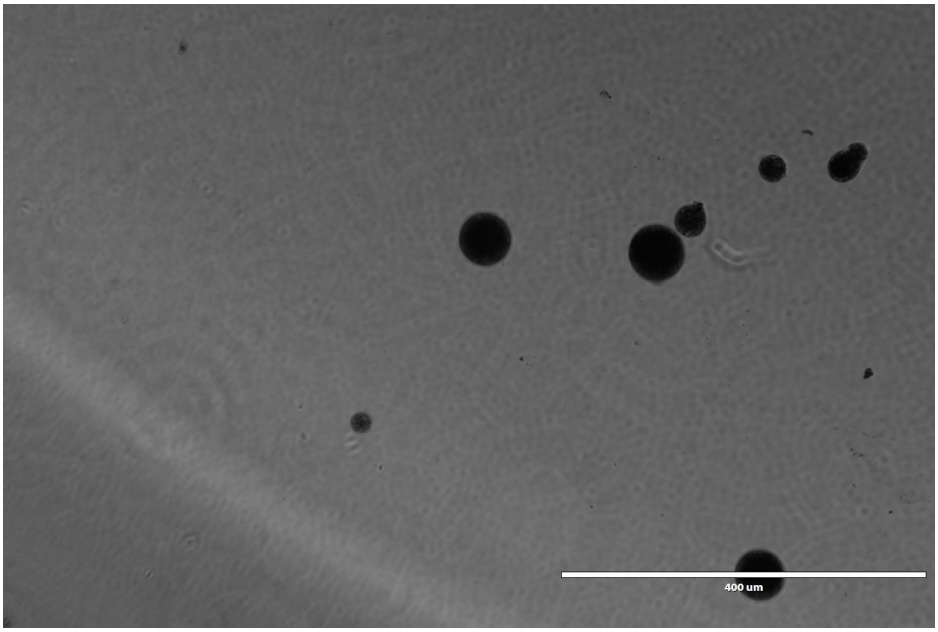

(a).

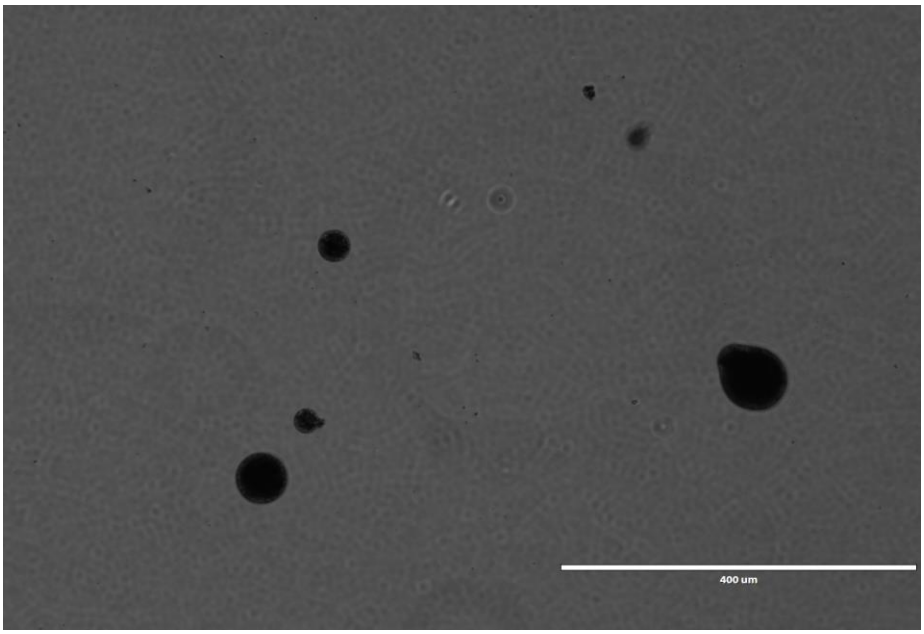

(b).

Figure 30. Images of magnetic beads at 10X magnification. (a). Magnetic beads irradiated at 740 nm. (b). Magnetic beads irradiated at 660 nm.